



Analysis of the systematic force-transmission error of the magnetic-suspension coupling in single-sinker densimeters and commercial gravimetric sorption analyzers

Reiner Kleinrahm¹ · Xiaoxian Yang² · Mark O. McLinden³ · Markus Richter⁴ 

Received: 22 September 2018 / Revised: 2 December 2018 / Accepted: 23 March 2019 / Published online: 23 April 2019
© Springer Science+Business Media, LLC, part of Springer Nature 2019

Abstract

Here we present an analysis of the force-transmission error for a commercial gravimetric sorption analyzer that applies equally to single-sinker densimeters. Gravimetric sorption analyzers are commonly used for the investigation of gas adsorption on porous materials (e.g., zeolites) with a simultaneous density measurement of the sample gas. The key component of the instrument is a magnetic-suspension coupling; this coupling transmits, without contact, the weight of the “density sinker” and of the sample container with the porous sample (which are both inside a pressurized measuring cell) to a balance at ambient pressure. However, since neither the coupling housing nor the sample gas are magnetically neutral, a small, systematic force-transmission error (FTE) occurs. For the correction of this FTE, an empirical correction model was developed. We show that the FTE can be subdivided into two parts: an apparatus contribution, and a fluid contribution. In the current paper we describe the effect of the FTE on the accuracy of the density measurements; the effect of the FTE on the accuracy of sorption measurements on porous and non-porous materials will be presented in a companion paper. The magnitude of the FTE in case of density measurement is shown by comparing the results of density measurements of four pure gases with values calculated from reference equations of state. The apparatus contribution of the FTE is typically $(0.23 \text{ kg m}^{-3} + 50 \times 10^{-6} \cdot \rho_{\text{fluid}})$, and the fluid contribution can reach values up to $500 \times 10^{-6} \cdot \rho_{\text{fluid}}$ for diamagnetic fluids; for oxygen-containing gas mixtures it can be much greater.

Keywords Gravimetric sorption analyzer · Single-sinker densimeter · Force-transmission error · Magnetic-suspension coupling · Tandem-sinker densimeter

Partial contribution of the National Institute of Standards and Technology. Not subject to copyright in the United States.

✉ Markus Richter
m.richter@mb.tu-chemnitz.de

- ¹ Thermodynamics, Ruhr University Bochum, Bochum 44780, Germany
- ² Fluid Science & Resources Division, The University of Western Australia, Crawley, WA 6009, Australia
- ³ Applied Chemicals and Materials Division, National Institute of Standards and Technology, 325 Broadway, Boulder, CO 80305, USA
- ⁴ Applied Thermodynamics, Chemnitz University of Technology, Chemnitz 09107, Germany

1 Introduction

A variety of instruments make use of a magnetic-suspension coupling (MSC) to perform gravimetric experiments. In combination with an analytical balance, it is also called a magnetic-suspension balance, where the MSC isolates the balance from a test sample contained within a closed measuring cell. Such instruments have been used for the development of densimeters for more than 30 years, and they are increasingly used in research for thermogravimetric or sorption analyses.

The principle of contactless weighing was developed by Clark (1947), and the first type of a MSC was developed by Gast (1963, 1967, 1969). The version described by Gast (1967, 1969) was also commercially available from

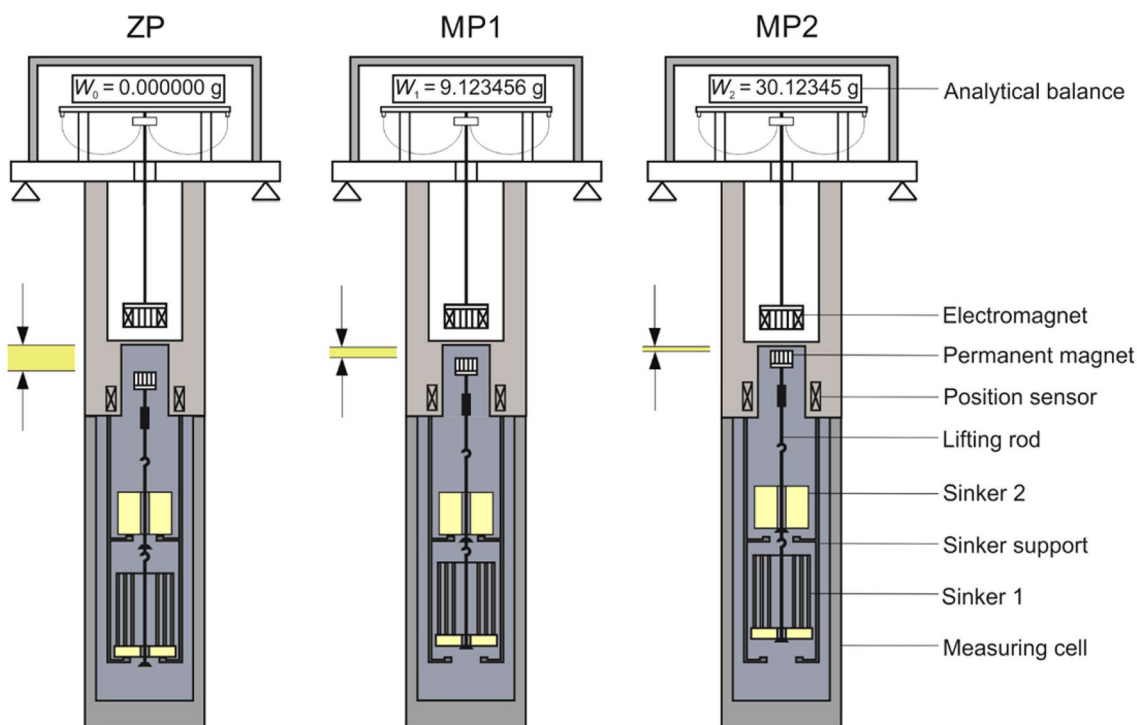


Fig. 1 Schematic representation of the three weighing positions of a gravimetric sorption analyzer or a “tandem-sinker densimeter” as we named it here; ZP: zero position or tare position, where only the permanent magnet and the lifting rod assembly is in suspension; MP1:

measuring position 1, where sinker 1 is lifted; MP2: measuring position 2, where both sinkers are lifted into suspension. The change in height of the permanent magnet between the positions ZP and MP1 and MP1 and MP2 is in both cases a few millimeters

Sartorius,¹ Germany, until the 1980s. In the early 1980s, a novel type of densimeter (a two-sinker densimeter) was developed by Kleinrahm and Wagner (1984, 1986) in which a modified version of Gast’s MSC was used; it was developed by Gast, Kleinrahm, Lösch, and Wagner. In the following years, the technique of MSCs has been decisively improved by Lösch (1987) and Lösch et al. (1994a, b), which allowed its application to density measurements at extreme conditions and with high accuracy. A review of the application of the MSC in densimeters (commonly referred to as single-sinker and two-sinker densimeters) was given by Wagner and Kleinrahm (2004) and McLinden (2015), and a list of selected single-sinker densimeters from the literature was provided by Yang et al. (2015). At present, a new four-sinker densimeter is under development in our group by Moritz et al. (2017).

The application of the MSC as a gravimetric sorption analyzer, or as a “tandem-sinker densimeter” as we name it here, was first developed by Dreisbach and Lösch in the

late 1990s and published by them in 2000; it measured both, the adsorption characteristics of a sample of porous material filled in a sample container and, by use of a density sinker, the density of the sample gas surrounding the porous material. Such gravimetric sorption analyzers have been commercially available from Rubotherm, Germany, since 1999.² Numerous applications of such analyzers to sorption experiments can be found in the literature (e.g., Dreisbach and Lösch 2000; May et al. 2001; Cavenati et al. 2004; Hefti et al. 2015). The key component is a MSC that transmits, without contact, the weight of the sample container and the density sinker from the pressurized measuring cell to a balance at ambient pressure. However, since both the coupling housing and the sample gas are not entirely magnetically neutral, a small force-transmission error (FTE) occurs. In the current paper, we present an analysis of the FTE for this type of instrument. First, the principle of the MSC and the commercial gravimetric sorption analyzer is described in Sect. 2. The difference to a single-sinker densimeter is also briefly explained there. Sect. 3 then deals with the FTE of the

¹ Commercial equipment, instruments, or materials are identified only in order to adequately specify certain procedures. In no case does such identification imply recommendation or endorsement by the National Institute of Standards and Technology, nor does it imply that the products identified are necessarily the best available for the purpose.

² Since September 2016, the company is a subsidiary of TA Instruments, USA.

MSC. In Sect. 4, we describe density measurements of four pure gases and synthetic air. Section 5 gives a brief summary of the results of sorption measurements of carbon dioxide on zeolite 13X; full details are presented in a companion paper (Yang et al. 2019). Finally, Sect. 6 presents brief conclusions.

2 Apparatus description

2.1 Measurement principle

The principle of the gravimetric sorption analyzer is illustrated in Fig. 1, where the key component is a MSC. The MSC comprises: (1) an electromagnet that is hung from the under-pan weighing hook of an electronic balance, (2) a permanent magnet together with a lifting rod for two sinkers, which are levitated by the electromagnet, and (3) a position sensor and feedback control circuit that makes fine adjustments in the electromagnet current to maintain the permanent magnet and the sinkers in stable suspension. By this arrangement, an MSC transmits the forces on the sample to the balance. The electromagnet and permanent magnet are separated by a pressure separating wall that isolates the sample (which may be at extremes of temperature or pressure) from the balance (which is at ambient conditions).

Usually, a “density sinker” is placed in the top position of the measuring cell, and a small sample-filled container is placed in the bottom position. The density sinker is used to determine the density of the sample gas, and the container filled with sample of an adsorbent material is used to determine the adsorption on the porous material. For the current analysis of the FTE, the sample container was replaced with a second density sinker, and we used the apparatus as a “tandem-sinker densimeter”. The two sinkers can be lifted by the lifting rod via the MSC. The MSC has three stable suspension positions: (1) a tare or zero position (ZP), where only the permanent magnet together with the lifting rod are in suspension, (2) a lower measuring position 1 (MP1), where the sinker at the bottom position is lifted up, and (3) an upper measuring position 2 (MP2), where both sinkers are lifted up. The three weighing positions are depicted in Fig. 1. Switching among the three positions is realized by vertical motion of the permanent magnet. The change in height of the permanent magnet between the positions ZP and MP1 and MP1 and MP2 is in both cases a few millimeters, depending primarily on the masses of the sinkers and, to a lesser degree, the temperature of the MSC. In contrast to the gravimetric sorption analyzer, the MSC of a single-sinker densimeter only has two stable suspension positions, a tare or ZP and a MP. Furthermore, only a single sinker is used for the density measurement of a sample fluid.

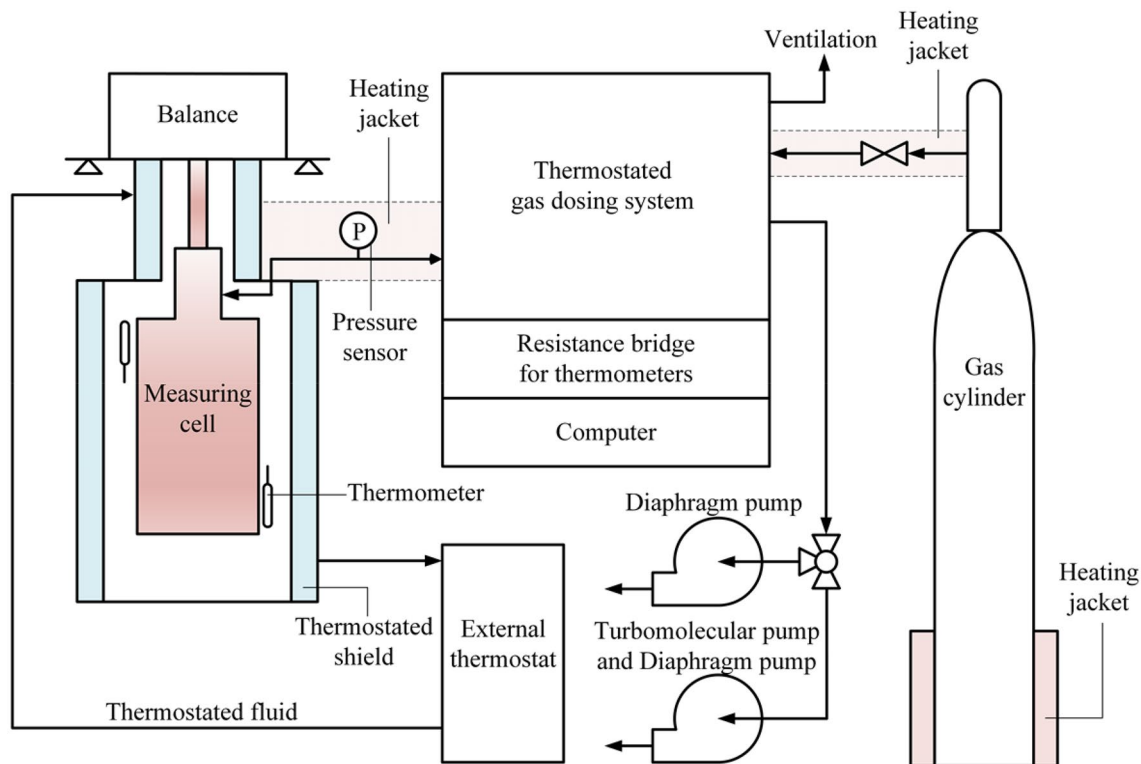


Fig. 2 Schematic diagram of the measuring system

2.2 Measurement system

Various types of gravimetric sorption analyzers are commercially available (see Sect. 1). The measurement system utilized in our group at Ruhr-Universität Bochum is schematically illustrated in Fig. 2. The original commercial instrument was modified in order to obtain greater repeatability and lower measurement uncertainty and to be capable of the analysis of the FTE for this work. These modifications included: (1) The original sinker lifting rods and sinker resting screws were changed to ensure a better alignment while lifting or depositing the sinkers; (2) The temperature and pressure measurement chains were improved and carefully calibrated; (3) Various sinkers were fabricated and their masses and volumes were well calibrated; (4) The original analytical balance (readability: 10 μg) was replaced with a microbalance (readability: 1 μg).

The core apparatus is accommodated in a frame with an analytical balance (Mettler-Toledo, Switzerland, type: WXS206SDU) at the top, followed by the MSC, and a measuring cell at the bottom. Both the MSC and the measuring cell are thermostated with an external circulating bath (Huber, Germany, type: K15). The core apparatus is connected to an automated, thermostated gas-dosing system, which was used to control the pressure inside the measuring cell. The sample gas cylinder and all the sample tubes exposed to the surroundings were thermostated to a temperature higher than the critical temperature of the sample gas to avoid condensation. A turbomolecular pump (Pfeiffer, Germany, type: HiCube 80 Eco), which can achieve a pressure lower than 0.001 Pa, was used to evacuate the measuring cell. The sorption analyzer operates over the temperature range from (283.15 to 423.15) K with pressures up to 35 MPa (although a smaller range of conditions are reported here).

The temperature was measured with a 100 Ω platinum resistance thermometer (Lake Shore, USA, type: PT-103) in conjunction with a resistance bridge (Anton Paar, Austria, type: MKT50) and the calibrated internal resistor (approximately 400 Ω) of the bridge. The thermometer was calibrated in-house on ITS-90 at the triple point of water (273.160 K), the melting point of gallium (302.9146 K), and the freezing point of indium (429.7485 K). The expanded uncertainty ($k=2$) in the temperature measurement due to the calibration of the thermometer was estimated to be 3.0 mK and that of the whole temperature measurement chain was 8.0 mK. A second thermometer was installed to estimate the temperature gradient across the whole measuring cell. With all uncertainty contributions (including temperature fluctuations during measurements) taken into consideration, the expanded uncertainty ($k=2$) in the temperature measurement was estimated to be 16 mK.

The pressure was measured with a vibrating quartz-crystal transducer (range up to 13.8 MPa, Paroscientific, USA, type: 42K-101). The transmitter and its connection tube to the main gas line (which connected the core apparatus and the gas-dosing system) were thermostated at $T \approx 333.15$ K to avoid condensation of the sample gas. The manufacturer specifies an expanded uncertainty ($k=2$) of 1.0×10^{-4} of full scale for the transducer, i.e., 1.38 kPa. In order to reduce this uncertainty, the pressure measurement chain was annually calibrated in-situ with a piston gauge (Fluke Calibration, USA, type: PG-7601), and the expanded uncertainty ($k=2$) in pressure measurement due to the calibration was estimated to be $5.0 \times 10^{-5} \cdot p$. The zero-point offset of the transducer was determined by evacuating the measuring cell before starting a new measurement run on an isotherm, and the display reading of the transducer at vacuum was subtracted from each pressure measurement. A hydrostatic head correction was applied to compensate for the differing heights of the pressure transducer and measuring cell. With all uncertainty contributions taken into consideration, the expanded uncertainty ($k=2$) in the pressure measurement was estimated to be between (0.2 and 0.7) kPa for the pressure range investigated here.

3 Analysis of the force-transmission error

The key component of the gravimetric sorption analyzer is the MSC, which was explained in Sect. 2.1. This coupling transmits, without contact, the weight of the sample container and the sinker in the pressurized measuring cell to a balance at ambient pressure. However, since both the coupling housing (that is, the upper part of the measuring cell) and the sample gas inside the measuring cell are not entirely magnetically neutral, a FTE occurs. The FTE of the coupling housing was first identified by Brachthäuser et al. (1993), and the FTE of the sample fluid was first identified by Klimeck (1997) and Klimeck et al. (1998); a brief summary was given by Wagner and Kleinrahm (2004). The reason for this FTE is the force interaction of the permanent magnet with the coupling housing, and this force interaction changes due to the movement of the permanent magnet between the positions ZP to MP1 and MP1 to MP2; in the higher positions MP1 and MP2 of the permanent magnet, the force interaction increases in comparison to the position ZP. This FTE is analyzed in the following subsections.

A comprehensive analysis of the FTE of MSCs utilized for single-sinker densimeters and two-sinker densimeters was presented by McLinden, Kleinrahm and Wagner (2007), and we use some of their results here. A slightly modified form of the analysis of McLinden et al. (2007) was used by Cristancho et al. (2010) to investigate the FTE

of their high-pressure (200 MPa) single-sinker densimeter. An alternative to the empirical approach of McLinden et al. (2007) was presented by Kuramoto et al. (2004). Their approach is based on a physical model, but it is complex and requires detailed knowledge of the magnetic properties of the apparatus and fluid, which may not be available. Another embodiment of the MSC was proposed by Kano et al. (2007) and realized by Kayukawa et al. (2012). There, the permanent magnet is held in a constant vertical position in both the tare and the measuring positions by moving the vertical position of the electromagnet. This technique significantly reduces the effect of the FTE and reduces the uncertainty in density, but it is very complex and is applicable only for specialized metrological applications.

For the following analysis of the FTE of a gravimetric sorption analyzer, we use the apparatus as “tandem-sinker densimeter”, i.e., we use a density sinker in the upper measuring position (MP2) and also in the lower measuring position (MP1). In this way, we illustrate the FTE with the MSC in the different positions, but the results are equally applicable when this type of instrument is used as a sorption analyzer with a single density sinker together with a sorption sample. For the set of investigations presented here, we use four different sinkers; two titanium sinkers (Ti20a and Ti20b, mass $m \approx 20$ g), a stainless steel sinker (SS14, $m \approx 14$ g), and another stainless steel sinker (SS09, $m \approx 9$ g). The three sinkers Ti20a, Ti20b, and SS14 are cylinders with a central bore for the sinker support. Sinker SS09 has a special form and is used as “sorption sinker”. The four sinkers are specified in Table 1.

The analysis of the FTE is presented in Sect. 3.1 to 3.5, and a summary for the application of the empirical correction model is given in Sect. 3.6.

3.1 Determination of the density of a sample fluid

In order to determine the density of a sample fluid, a sinker of known mass and known volume is weighed in the sample gas within the measuring cell. Hence, the weighing result is the difference between the mass of the sinker and the buoyancy of the gas on the sinker:

$$(W_2 - W_1)_{\text{fluid}} = (m_S - \rho_{\text{fluid}} \times V_S) \times \alpha \times \phi, \tag{1}$$

where W_1 and W_2 are the balance readings at the measuring positions MP1 and MP2, m_S and V_S are the mass and volume of the sinker, ρ_{fluid} is the density of the sample fluid, α is the balance calibration factor, and ϕ is the coupling factor, which accounts for the FTE of the MSC. Equation (1) was written for the upper sinker, but it can be applied analogously for the bottom sinker with $(W_1 - W_{ZP})_{\text{fluid}}$. At the beginning of each measurement run, the balance is usually tared (i.e., balance reading: $W_{ZP} = 0.000000$ g).

Since balances are generally calibrated in air with internal standard masses, they will read “10.000000 g” when weighing a 10 g standard mass, even though the weighing is affected by air buoyancy. The balance calibration factor α accounts for this fact:

$$\alpha = 1 / (1 - \rho_{\text{air}} / \rho_{\text{calib}}), \tag{2}$$

where $\alpha \approx 1.000150$ for a typical sea-level air density of $\rho_{\text{air}} \approx 1.20 \text{ kg m}^{-3}$, and stainless steel calibration masses with a density of $\rho_{\text{calib}} \approx 8000 \text{ kg m}^{-3}$. Calibration of the balance should be carried out at the beginning of each measurement run.

The FTE due to the MSC can be subdivided into two parts, an apparatus contribution, ϵ_{vac} , and a fluid contribution, ϵ_{fluid} .

Table 1 Specification of the four sinkers used

Sinker	Material	m/g	$10^6 \times U(m)/m$	V_0/cm^3	$10^6 \times U(V_0)/V_0$	A/cm^2
Ti20a ^a	Titanium	19.65711	20	4.360347	10	18.1
Ti20b ^a	Titanium	19.63806	30	4.367245	80	18.1
SS14 ^a	SS304 ^c	14.00420	40	1.771903	30	10.2
SS09 ^b	SS304 ^c	9.32721	60	1.177403	200	89.2

The masses and volumes of the sinkers Ti20a and SS14 were determined at NIST, while the masses and volumes of the sinkers Ti20b and SS09 were determined at Ruhr-Universität Bochum. $U(m)/m$ and $U(V_0)/V_0$ are the relative expanded uncertainty ($k=2$) of the mass and the volume, respectively. V_0 is the volume of the sinker at reference state ($p_0 = 0.101325$ MPa and $T_0 = 293.15$ K). A is the estimated geometrical surface area of the sinker

^aCylinder with outer diameter d_o , concentric inner diameter d_i , and height h : Ti20a: $d_o = 18.2$ mm, $d_i = 5.0$ mm, $h = 18.2$ mm; surface polished with abrasive to obtain a smoother finish. Ti20b: $d_o = 18.2$ mm, $d_i = 5.0$ mm, $h = 18.2$ mm; surface left “as machined”. SS14: $d_o = 18.2$ mm, $d_i = 5.0$ mm, $h = 7.4$ mm; surface left “as machined”

^bSorption sinker with a base ring $d_o = 20.0$ mm, $d_i = 5.0$ mm, $h = 6.0$ mm, and three upper rings: thickness 0.1 mm, $d_o = (11.0, 15.0, 19.0)$ mm, and $h = 27.0$ mm (see Fig. 1, bottom sinker). No special treatment was applied to the surface of this sinker. The base ring was made on a lathe, and the upper rings were made on a rolling machine

^cType 1.4301 stainless steel (equivalent to SAE/ANSI type 304)

The coupling factor ϕ accounts for this FTE and can be defined as follows:

$$\phi = 1 + \varepsilon_{\text{vac}} + \varepsilon_{\text{fluid}}. \quad (3)$$

The two FTE contributions, ε_{vac} and $\varepsilon_{\text{fluid}}$, are explained in the Sect. 3.3 and 3.4, respectively. Their values range from $(-27 \text{ to } -59) \times 10^{-6}$ for ε_{vac} and from $(0 \text{ to } 30) \times 10^{-6}$ for $\varepsilon_{\text{fluid}}$ depending on the position of the sinker (bottom or top) and its mass. These values apply to our present instrument; they will be different for other instruments.

The fluid contribution of the FTE, $\varepsilon_{\text{fluid}}$, is approximately proportional to the specific susceptibility and the density of the sample gas as demonstrated by McLinden et al. (2007):

$$\varepsilon_{\text{fluid}} = \varepsilon_{\rho} \times (\chi_s / \chi_{s0}) \times (\rho_{\text{fluid}} / \rho_0), \quad (4)$$

where ε_{ρ} is the constant of proportionality, χ_s is the specific magnetic susceptibility of the sample gas, $\chi_{s0} = 10^{-8} \text{ m}^3 \text{ kg}^{-1}$ is a reducing constant, ρ_{fluid} is the density of the sample fluid, and $\rho_0 = 1000 \text{ kg m}^{-3}$ is also a reducing constant.

In order to reduce the number of symbols, we define:

$$m_{\text{S,fluid}}^* = (W_2 - W_1)_{\text{fluid}} / \alpha \quad (5)$$

and

$$m_{\text{S,vac}}^* = (W_2 - W_1)_{\text{vac}} / \alpha, \quad (6)$$

where $(W_2 - W_1)_{\text{fluid}}$ is the weighing “value” of the sinker (via the MSC) immersed in the sample fluid. By integrating the balance calibration factor α , we get the weighing “result” $m_{\text{S,fluid}}^*$ (in mass units). (In the literature, this value is often referred to as “apparent mass” of the sinker immersed in a fluid, e.g., May et al. (2001)). Likewise, $(W_2 - W_1)_{\text{vac}}$ is the weighing “value” of the sinker in the evacuated measuring cell and $m_{\text{S,vac}}^*$ is the weighing “result”. In order to calculate average values with higher accuracy, the values $m_{\text{S,fluid}}^*$ and $m_{\text{S,vac}}^*$ should be measured several times in a measurement run.

Combining Eq. (1) with Eqs. (3) and (5) yields:

$$m_{\text{S,fluid}}^* = (m_{\text{S}} - \rho_{\text{fluid}} \times V_{\text{S}}) \times (1 + \varepsilon_{\text{vac}} + \varepsilon_{\text{fluid}}), \quad (7)$$

and combining Eq. (1) with Eqs. (3) and (6) yields:

$$m_{\text{S,vac}}^* = m_{\text{S}} \times (1 + \varepsilon_{\text{vac}}). \quad (8)$$

Subtracting Eq. (7) from Eq. (8) gives:

$$(m_{\text{S,vac}}^* - m_{\text{S,fluid}}^*) = -m_{\text{S}} \times \varepsilon_{\text{fluid}} + \rho_{\text{fluid}} \times V_{\text{S}} \times (1 + \varepsilon_{\text{vac}} + \varepsilon_{\text{fluid}}), \quad (9)$$

and with $m_{\text{S}} = V_{\text{S}} \times \rho_{\text{S}}$, where ρ_{S} is the density of the sinker, follows:

$$(m_{\text{S,vac}}^* - m_{\text{S,fluid}}^*) = \rho_{\text{fluid}} \times V_{\text{S}} \times [1 + \varepsilon_{\text{vac}} + \varepsilon_{\text{fluid}} \times (1 - \rho_{\text{S}} / \rho_{\text{fluid}})]. \quad (10)$$

By rearranging Eq. (10) and with $\varepsilon_{\text{fluid}}$ according to Eq. (4), the density of a sample fluid in the measuring cell can be determined by:

$$\rho_{\text{fluid}} = \frac{m_{\text{S,vac}}^* - m_{\text{S,fluid}}^*}{V_{\text{S}}} \times [1 + \varepsilon_{\text{vac}} + \varepsilon_{\rho} \times (\chi_s / \chi_{s0}) \times (\rho_{\text{fluid}} / \rho_0 - \rho_{\text{S}} / \rho_0)]^{-1}. \quad (11)$$

The last term in the brackets of Eq. (11) can now be rearranged and defined by:

$$\varepsilon_{\text{fse}} = \varepsilon_{\rho} \times (-\chi_s / \chi_{s0}) \times (\rho_{\text{S}} / \rho_0 - \rho_{\text{fluid}} / \rho_0). \quad (12)$$

We call this value, ε_{fse} , the “fluid-specific effect”; it is the fluid contribution of the FTE for single-sinker densimeters and gravimetric sorption analyzers only (see also last term in Eq. (10): $\varepsilon_{\text{fse}} = \varepsilon_{\text{fluid}} \times (1 - \rho_{\text{S}} / \rho_{\text{fluid}})$). Please note that for two-sinker densimeters (see references in Sect. 1), the term ρ_{S} / ρ_0 does not exist in Eq. (12); see also Eq. (4). Inserting ε_{fse} into Eq. (11) yields now the final result for determining the fluid density:

$$\rho_{\text{fluid}} = \frac{m_{\text{S,vac}}^* - m_{\text{S,fluid}}^*}{V_{\text{S}}} \times (1 + \varepsilon_{\text{vac}} + \varepsilon_{\text{fse}})^{-1}. \quad (13)$$

To calculate the fluid density with Eq. (13), the following three steps are necessary: (1) A preliminary value of ρ_{fluid} has to be determined according to Eq. (13) with $\varepsilon_{\text{vac}} = 0$ and $\varepsilon_{\text{fse}} = 0$; (2) The value ε_{fse} has to be determined according to Eq. (12) with the preliminary value of ρ_{fluid} ; (3) Finally, the fluid density ρ_{fluid} can be determined with Eq. (13). For most applications, Eq. (13) can be slightly simplified (see Appendix A1, Annotation A1).

It should be noted here that it is very important to use the value $m_{\text{S,vac}}^*$ according to Eq. (6) in Eq. (13) instead of the (actual) mass of the sinker m_{S} , otherwise the FTE of the term $m_{\text{S}} \cdot \varepsilon_{\text{vac}}$ (see Eq. (8)) would cause large errors, as explained in Sect. 3.2.

The density of a sample fluid in a gravimetric sorption analyzer is usually determined by a titanium sinker (mass $m_{\text{S}} \approx 20 \text{ g}$, volume $V_{\text{S}} \approx 4.4 \text{ cm}^3$) in the upper suspension position. A sorption sinker or a sample container with porous material is usually located in the lower position.

3.2 Explanation of the cause of the force-transmission error

The error in density of the sample fluid $\Delta\rho_{\text{FTE}}$ due to the FTE of the MSC can be determined as: $\Delta\rho_{\text{FTE}} = (\rho_{\text{fluid,uncorr}} - \rho_{\text{fluid}})$. The derivation for calculating the value $\Delta\rho_{\text{FTE}}$ is given in Appendix A1, Annotation 2. The result is a simple equation:

$$\Delta\rho_{\text{FTE}} \times V_{\text{S}} = -(\varepsilon_{\text{vac}} + \varepsilon_{\text{fluid}}) \times (m_{\text{S}} - \rho_{\text{fluid}} \times V_{\text{S}}), \quad (14)$$

where $\Delta\rho_{\text{FTE}} \times V_S = \Delta m_{\text{FTE}}$ corresponds to the FTE in mass units.

It can clearly be seen in Eq. (14) that the FTE is proportional to the mass of the sinker m_S , reduced by the buoyancy $\rho_{\text{fluid}} \times V_S$ on the sinker, and ϵ_{vac} (apparatus contribution) and ϵ_{fluid} (fluid contribution) are the factors of proportionality. Hence, Eq. (14) yields the FTE of the MSC in mass units. The values ϵ_{vac} and ϵ_{fluid} are individual factors, of course, for one sinker and in one of the two positions only, top or bottom. The mass value $(m_S - \rho_{\text{fluid}} \times V_S)$ in Eq. (14), i.e., the load that must be lifted by the MSC, corresponds to a change in height of the permanent magnet within its (magnetic) surroundings. For example, the sinker Ti20a (see Table 1) has a mass of $m_S \approx 20$ g, and the buoyancy of a sample gas with $\rho_{\text{fluid}} \approx 0.10$ g cm³ on the sinker volume $V_S \approx 4.4$ cm³ yields $\rho_{\text{fluid}} \times V_S \approx 0.44$ g. This mass difference $\Delta m \approx 19.56$ g, which must then be lifted by the MSC, is proportional to the height change of a few millimeters of the permanent magnet between the measuring positions MP1 and MP2 (or also between ZP and MP1) and, therefore, the force interaction between the permanent magnet and the coupling housing changes. (Please note that for two-sinker densimeters, the term m_S does not exist in Eq. (14)).

By far the greatest part of the FTE is caused by the term $m_S \cdot \epsilon_{\text{vac}}$ in Eq. (14). In comparison to this, the influence of the term $m_S \cdot \epsilon_{\text{fluid}}$ is usually much smaller because the value ϵ_{fluid} is proportional to the density of the sample fluid ρ_{fluid} , see Eq. (4). Therefore, it is very important to use the value $m_{S,\text{vac}}^*$ according to Eq. (8) in Eq. (13) instead of the (actual) mass of the sinker m_S , otherwise the FTE term $m_S \cdot \epsilon_{\text{vac}}$ would

cause large errors. For example, with $m_S \approx 20$ g, $V_S \approx 4.4$ cm³ and $\epsilon_{\text{vac}} \approx 50 \times 10^{-6}$ ($m_S \cdot \epsilon_{\text{vac}} \approx 1.0$ mg), a large error in density of about 0.23 kg m⁻³ would occur. For low densities, e.g., $\rho_{\text{fluid}} = 10$ kg m⁻³, this error corresponds to a relative error of 2.3%. Therefore, it is very important to determine the value $m_{S,\text{vac}}^*$ (see Eq. (6)) very carefully.

In order to obtain accurate results, it is necessary to correct the FTE caused by the magnetic suspension coupling. When the best achievable accuracy is not needed, the terms ϵ_{vac} and ϵ_{fse} in Eq. (13) can be omitted. (But note that the values $m_{S,\text{vac}}^*$ and $m_{S,\text{fluid}}^*$ are still used.) In this case, the FTE should be estimated and taken into account in the uncertainty analysis of the measurement. For example, the apparatus contribution ϵ_{vac} of the FTE in the present case is less than 60×10^{-6} (see Table 2). Since the fluid-specific effect ϵ_{fse} of the FTE can reach values up to 500×10^{-6} even for diamagnetic fluids, this effect should be estimated. For oxygen-containing gas mixtures, however, this value can be much greater and should be considered carefully (see Sect. 3.5). The results of this FTE analysis are also very useful for single-sinker densimeters.

3.3 Apparatus contribution of the force-transmission error

The apparatus contribution of the FTE, which we term ϵ_{vac} , is due to the magnetic properties of the coupling housing, as well as the magnetic components in its vicinity. It can be obtained by careful determination of the value $m_{S,\text{vac}}^*$ (see Eq. (6)) of the sinker in the evacuated measuring cell weighed via the MSC:

$$\epsilon_{\text{vac}} = (m_{S,\text{vac}}^* - m_S) / m_S. \tag{15}$$

This equation corresponds to a rearrangement of Eq. (8). The magnitude of the apparatus contribution of the FTE, ϵ_{vac} , depends on the magnetic properties of the material of the coupling housing and the components in its vicinity; ϵ_{vac} values are positive for diamagnetic coupling housings and negative for paramagnetic ones. These facts are discussed in more detail in Appendix A1, Annotation 3.

For the apparatus used in the present work, the ϵ_{vac} values range from $(-27$ to $-59) \times 10^{-6}$, depending on the position of the sinker (bottom or top) and its mass. In Table 2, the results are listed for the four sinkers, Ti20a, Ti20b, SS14, and SS09, at $T \approx 293.15$ K, where each sinker was weighed in the bottom and in the top positions and in different combinations. It can be seen that the values of the bottom position of the sinkers are much smaller than that for the top position and that the values increase with increasing mass. This is because the distance between the permanent magnet and the electromagnet in the MSC decreases as the load increases, leading to a steadily increasing magnetic field and

Table 2 Weighing values $m_{S,\text{vac}}^*$ of the four sinkers Ti20a, Ti20b, SS14, and SS09 in the evacuated measuring cell at $T \approx 293.15$ K

Bottom sinker			Top sinker		
Sinker ^a	$m_{S,\text{vac}}^*/\text{g}$	$\epsilon_{\text{vac}} \times 10^6$	Sinker ^a	$m_{S,\text{vac}}^*/\text{g}$	$\epsilon_{\text{vac}} \times 10^6$
Ti20b	19.63733	-37.2	Ti20a	19.65604	-54.4
Ti20a	19.65636	-37.9	SS14	14.00338	-58.6
Ti20a	19.65639	-36.4	SS09	9.32666	-58.9
SS14	14.00366	-38.3	Ti20a	19.65599	-56.9
SS14	14.00373	-33.1	SS09	9.32667	-58.2
SS09	9.32695	-28.6	Ti20a	19.65609	-51.8
SS09	9.32696	-27.3	SS14	14.00343	-55.0

Each sinker was measured in the bottom and in the top position, and in different combinations. The weighing value $m_{S,\text{vac}}^*$ is explained in Sect. 3.1 (Eq. 6) and the apparatus contribution ϵ_{vac} of the force-transmission error is defined in Sect. 3.3 (Eq. 15)

The measurements were carried out several times within 2 weeks. The measured values of $m_{S,\text{vac}}^*$ scattered within $\pm 0.0004\%$, which corresponds to a scattering of ϵ_{vac} of $\pm 4.0 \times 10^{-6}$

^aThe specifications of the four sinkers are listed in Table 1

a stronger magnetic interaction of the permanent magnet with surrounding materials. Hence, the measured values ε_{vac} are average values between the measuring positions ZP and MP1 and between MP1 and MP2. The measurements for the determination of ε_{vac} were carried out several times within two weeks, with the values showing a scatter of $\pm 4.0 \times 10^{-6}$. Therefore, we recommend to determine the value $m_{\text{S,vac}}^*$ at the beginning of each measurement run or immediately after, and this is absolutely necessary for accurate measurements. Based on the scatter, the standard uncertainty of ε_{vac} was estimated to be 4.0×10^{-6} . Please note that if the MSC is readjusted/realigned (e.g., due to relocation of the apparatus) and the position of the permanent magnet in the coupling housing is thus changed in the vertical and/or horizontal direction, the value ε_{vac} can change up to approximately $\pm 10 \times 10^{-6}$. For commercial sorption analyzers, two ε_{vac} values are needed, one for the titanium density sinker in the top position and one for the sample container with the porous sample in the bottom position.

3.4 Fluid contribution of the force-transmission error

Like metals, fluids also have magnetic properties. Therefore, the magnetic field of the MSC is influenced by the sample fluid inside the measuring cell. Due to the movement of the permanent magnet from the positions ZP to MP1 and MP1 to MP2, the force interaction between the permanent magnet and the coupling housing changes. This fluid contribution of the FTE, $\varepsilon_{\text{fluid}}$, (see Eq. (3)) is approximately proportional to the specific susceptibility and the density of the sample fluid; the relationship has already been introduced as Eq. (4) and was briefly explained. Equation (4) is an effective empirical approach that was developed by McLinden, Kleinrahn and Wagner (2007); it is well illustrated in their paper by three diagrams (Figs. 2, 3, 4) and by Eq. (13).

For gravimetric sorption analyzers (or tandem-sinker densimeters) and single-sinker densimeters, the “fluid-specific effect” of the FTE, ε_{fse} , is represented by Eq. (12), and was already defined in Sect. 3.1. The value ε_{ρ} in Eq. (12) is an apparatus-specific constant; its determination is explained in Sect. 3.5.

Most common pure fluids are diamagnetic, e.g., methane, ethane, nitrogen, argon, and carbon dioxide with specific magnetic susceptibilities (negative values for diamagnetic substances) at $T \approx 293.15$ K of $\chi_s/\chi_{s0} = -1.36, -1.12, -0.54, -0.61,$ and -0.60 , respectively, where $\chi_{s0} = 10^{-8} \text{ m}^3 \text{ kg}^{-1}$ is a reducing constant (CRC Handbook 2016). The susceptibility of diamagnetic fluids varies only slightly with temperature (CRC Handbook 2016). An equation for calculating the specific susceptibility of gas mixtures is described in Appendix A2. In contrast to diamagnetic fluids, the susceptibility of paramagnetic fluids is much greater and shows a much

stronger temperature dependence, varying roughly as $1/T$ (CRC Handbook 2016). The most common paramagnetic fluids are oxygen and oxygen-containing mixtures, in particular air. The specific susceptibilities of oxygen and air are given in the next Sect. 3.5 and in Appendix A3.

3.5 Determination of the apparatus-specific constant ε_{ρ}

Two methods for determining the apparatus-specific constant ε_{ρ} were already explained by McLinden et al. (2007). A simple approach is the density measurement of pure oxygen, e.g., at $T \approx 293.15$ K and $p \approx 0.1$ MPa (but at most at $p \approx 1$ MPa), because the specific susceptibility of (paramagnetic) oxygen is very large, $\chi_s/\chi_{s0} = +134.13$ at $T = 293.15$ K (May et al. 2008). However, in most cases commercial gravimetric sorption analyzers are not suitable for measurements of pure oxygen. Therefore, the safest approach is the density measurement of synthetic air; its specific susceptibility is approximately $\chi_s/\chi_{s0} \approx +30.74$ at $T = 293.15$ K and thus still relatively large. The specific susceptibilities of oxygen and synthetic air are further discussed in Appendix A3.

For the apparatus used here, the apparatus-specific constant ε_{ρ} was determined on the basis of density measurements on synthetic air (0.2094 ± 0.0020 mol fraction oxygen in nitrogen; specific susceptibility $\chi_s/\chi_{s0} \approx 30.74$ at $T = 293.15$ K). The procedure for these density measurements is explained in Sect. 4. The results of the measurements with the Ti20a and the SS14 sinkers in the top and the bottom position are listed in Table 3. The experimental densities were calculated according to Eq. (13) but with $\varepsilon_{\text{fse}} = 0$, i.e., without correction of the fluid-specific effect. The relative deviations of these uncorrected experimental densities, called $\rho_{\text{exp,uncorr}}$ from reference values ρ_{GERG} calculated with the GERG-2008 equation of state (Kunz and Wagner 2012) are also listed in Table 3 and they are plotted in Fig. 3. The relative deviations of (-0.5 to -2.2)% are equal to the fluid-specific effect for the synthetic air sample:

$$\varepsilon_{\text{fse}} = (\rho_{\text{exp,uncorr}} - \rho_{\text{GERG}}) / \rho_{\text{GERG}} \quad (16)$$

Based on these relative deviations $(\rho_{\text{exp,uncorr}} - \rho_{\text{GERG}}) / \rho_{\text{GERG}}$, which corresponds to the experimental value ε_{fse} , the apparatus-specific constant ε_{ρ} can be determined by rearranging Eq. (12):

$$\varepsilon_{\rho} = \varepsilon_{\text{fse}} \times (-\chi_s/\chi_{s0})^{-1} \times (\rho_{\text{S}}/\rho_0 - \rho_{\text{fluid}}/\rho_0)^{-1} \quad (17)$$

For this determination, a single deviation value ε_{fse} according to Eq. (16) at a high density ρ_{exp} could be used; the results for the constant ε_{ρ} are also listed in Table 3. In this case, the uncertainty of the GERG-2008 equation must be taken into account, which was reported by the authors to

Table 3 Measurements of the density $\rho_{\text{exp,uncorr}}$ of synthetic air and determination of the apparatus specific constant ϵ_ρ , where T is the temperature (ITS-90), p is the pressure, and $\Delta\rho/\rho = 100 \times (\rho_{\text{exp,uncorr}} - \rho_{\text{GERG}})/\rho_{\text{GERG}}$, which are the relative deviations of the experimental densities $\rho_{\text{exp,uncorr}}$ from values ρ_{GERG} calculated with the GERG-2008 equation of state (Kunz and Wagner 2012)

T/K	p/MPa	$\rho_{\text{GERG}}/(\text{kg m}^{-3})$	$\rho_{\text{exp,uncorr}}^a/(\text{kg m}^{-3})$	$\Delta\rho/\rho$	$\epsilon_\rho^b \times 10^6$	$\rho_{\text{exp,uncorr}}^a/(\text{kg m}^{-3})$	$\Delta\rho/\rho$	$\epsilon_\rho^b \times 10^6$
			Bottom sinker SS14			Top sinker Ti20a		
293.203	1.9967	23.7553	23.5215	-0.984	41	23.5112	-1.027	75
293.207	3.9873	47.6338	47.1834	-0.946	39	47.1581	-0.999	73
293.197	6.0087	71.9495	71.2826	-0.927	39	71.2443	-0.980	72
293.199	7.9870	95.6591	94.7918	-0.907	38	94.7417	-0.959	71
293.190	6.0597	72.5652	71.8924	-0.927	39	71.8554	-0.978	72
293.192	4.0436	48.3141	47.8544	-0.951	40	47.8306	-1.001	74
293.190	2.0146	23.9694	23.7322	-0.989	41	23.7221	-1.032	75
			Bottom sinker Ti20a			Top sinker SS14		
293.217	1.9898	23.6713	23.5403	-0.553	40	23.1655	-2.137	89
293.223	3.9877	47.6371	47.3839	-0.531	39	46.6410	-2.091	87
293.215	5.9874	71.6888	71.3204	-0.514	38	70.2124	-2.059	86
293.211	8.0068	95.8904	95.4139	-0.497	37	93.9429	-2.031	85
293.194	6.0667	72.6476	72.2737	-0.515	38	71.1503	-2.061	86
293.198	4.0281	48.1268	47.8704	-0.533	39	47.1179	-2.096	87
293.198	2.0123	23.9419	23.8080	-0.559	41	23.4276	-2.148	89

The presented measurements were carried out with the Ti20a and the SS14 sinkers (see Table 1) in both the bottom and the top position. Note: The Ti20a sinker is usually in the upper position while another sinker or a sample container is in the lower position. We have changed the positions of the two sinkers only to demonstrate the effects on the apparatus-specific constant ϵ_ρ

The expanded uncertainties ($k=2$) of the measurements are 16 mK for temperature, between (0.2 and 0.7) kPa for pressure, and 0.020 kg m⁻³ for density. The composition of the synthetic air is (0.2094 ± 0.0020) mole fraction oxygen in nitrogen; see Table 5

^aThe experimental densities $\rho_{\text{exp,uncorr}}$ were calculated according to Eq. (13) with $\epsilon_{\text{fse}}=0$, i.e., without correction of the fluid-specific effect

^bThe values of ϵ_ρ were calculated according to Eq. (17). The extrapolation of the experimental densities of the Ti20a sinker in the top position to $\rho_{\text{exp,uncorr}}=0$ yields $\epsilon_\rho \times 10^6 = 76$. The extrapolation of the values ϵ_ρ to $\rho_{\text{exp,uncorr}}=0$ yields the same result

be less than or equal to 0.3% for the region considered here (but we assume it is less than 0.05%). However, a much more accurate constant ϵ_ρ can be determined by extrapolation of several density measurements to the density $\rho_{\text{fluid}}=0$ (see Fig. 3) because the uncertainty of the GERG-2008 equation is zero in the ideal gas limit. The results determined in this way are listed in Table 4 for the four sinkers in different combinations. For the apparatus used here, the values for ϵ_ρ range from (36 to 97) × 10⁻⁶, depending on the position of the sinker (bottom or top) and its mass; for sinkers in the lower position, the constants ϵ_ρ are much smaller than for sinkers in the upper position. (The reason for this behavior was briefly explained in Sect. 3.3 for the value ϵ_{vac} .) The temperature dependence of ϵ_ρ was less than 2 × 10⁻⁶ for a change from $T \approx 293.15$ to $T \approx 323.15$ K.

The Ti20a sinker is usually used in the top position for the density measurement of the sample fluid. By extrapolation of these results listed in Table 3 to the density $\rho_{\text{fluid}}=0$, the deviation from the value calculated with the GERG-2008 equation yields $(\rho_{\text{exp,uncorr}} - \rho_{\text{GERG}})/\rho_{\text{GERG}} = \epsilon_{\text{fse}} = -1.051\%$. With this value and with $\chi_s/\chi_{s0} \approx +30.74$ (at $T \approx 293.200$ K)

and $\rho_s/\rho_0 = 4.51$, the apparatus-specific constant ϵ_ρ was determined according to Eq. (17) with the result $\epsilon_\rho = (76 \pm 5) \times 10^{-6}$; its expanded uncertainty ($k=2$) was estimated to be 6% for the sorption analyzer used, based on the uncertainty of the density measurement on the synthetic air sample and the uncertainty of the extrapolation of these measurements to $\rho_{\text{fluid}}=0$.

The fluid-specific effect ϵ_{fse} of the FTE can now be determined with Eq. (12). The expanded uncertainty ($k=2$) of this value ϵ_{fse} was conservatively estimated to be 10%, which includes: (1) the uncertainty of the apparatus-specific constant ϵ_ρ , (2) the uncertainty of the fluid composition (e.g. air), (3) the uncertainty of the specific susceptibility of the fluid sample (e.g. air), and (4) the estimated uncertainty of the empirical approach of the model term ϵ_{fse} . The determined value for ϵ_{fse} can now be used to correct the fluid-specific effect of diamagnetic and paramagnetic pure fluids and mixtures, including oxygen-containing mixtures with oxygen mole fractions up to about 0.20. Additional information about this point and about the apparatus-specific constant ϵ_ρ are given in Appendix A1, Annotation 4.

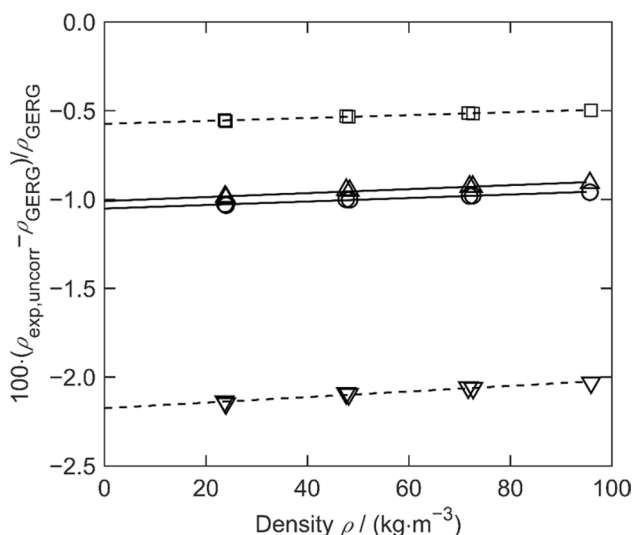


Fig. 3 Relative deviations of the experimental densities $\rho_{\text{exp,uncorr}}$ for synthetic air at $T \approx 293.15$ K from values ρ_{GERG} calculated with the GERG-2008 equation of state (Kunz and Wagner 2012); see Table 3. The experimental density $\rho_{\text{exp,uncorr}}$ were calculated according to Eq. (13) with $\varepsilon_{\text{fse}}=0$, i.e., without correction of the fluid-specific effect. (open circle) and (open triangle), measurement with the Ti20a sinker in the top position and the SS14 sinker in the bottom position, respectively; (open square) and (open inverted triangle), measurement with the Ti20a sinker in the bottom position and the SS14 sinker in the top position, respectively; see Table 3 and Sect. 3.5. Thus, the deviations represent the fluid-specific effect ε_{fse} according to Eq. (16). Based on these relative deviations, the apparatus constant ε_{ρ} can be determined by Eq. (17). The Ti20a sinker is usually in the upper position while another sinker or a sample container is in the lower position. We have changed the positions of the two sinkers only to demonstrate the effects on the apparatus-specific constant ε_{ρ}

Table 4 Determination of the apparatus-specific constant ε_{ρ} with various sinkers and in different combinations at $T \approx 293.15$ K

Bottom sinker		Top sinker	
Sinker	$\varepsilon_{\rho} \times 10^6$	Sinker	$\varepsilon_{\rho} \times 10^6$
Ti20a	38	Ti20b	81
Ti20a	39	SS14	89
Ti20a	39	SS09	97
SS14	39	Ti20a	74
SS14	39	SS09	87
SS09	36	Ti20a	68
SS09	37	SS14	74

The constants ε_{ρ} were determined by extrapolation of several density measurements to the density $\rho_{\text{fluid}}=0$ (see explanation in Sect. 3.5). The needed measurements were conducted with synthetic air, (0.2094 \pm 0.0020) mole fraction oxygen in nitrogen, with pressures from (2.0 to 8.0) MPa; see also Table 3

For commercial sorption analyzers, two ε_{ρ} values are needed, one for the titanium density sinker in the top position and one for the sample container with the porous sample

in the bottom position. The value ε_{ρ} for a sample-filled container, however, cannot be determined in synthetic air. Therefore, instead of the porous sample in the container, a solid metal piece with approximately the same mass can be used. Additional information are given in Appendix A1, Annotation 5.

3.6 Summary for the application of the empirical correction model

To implement the correction model presented in Sect. 3.1 to 3.5, the following steps should be implemented in the data analysis:

- (1) The density of the sample fluid can be determined by Eq. (13).
- (2) The weighing “results” $m_{\text{S,fluid}}^*$ and $m_{\text{S,vac}}^*$ of the sinkers can be determined by Eqs. (5) and (6), respectively, and the balance calibration factor α can be calculated by Eq. (2).
- (3) The density of a sample fluid in a gravimetric sorption analyzer is usually determined by a titanium sinker (mass $m_{\text{S}} \approx 20$ g, volume $V_{\text{S}} \approx 4.4$ cm³) in the upper suspension position. The volume change of a titanium sinker with temperature and pressure $V_{\text{S}}(T, p)$ is described in Appendix A4.
- (4) The value ε_{vac} (apparatus contribution of the FTE) can be determined by Eq. (15).
- (5) The value ε_{fse} (called “fluid-specific effect”, which is the fluid contribution of the FTE for gravimetric sorption analyzers) can be determined by Eq. (12). The required value ε_{ρ} is described in the next item 6. The needed values of the specific magnetic susceptibility χ_{S} of the sample gas are given in Appendices 2 and 3. The density ρ_{S} of the sinker used, e.g. a titanium sinker, is $\rho_{\text{S}} \approx 4510$ kg m⁻³ (see Table 1) where $\rho_0 = 1000$ kg m⁻³ is a reducing constant.
- (6) The apparatus-specific constant ε_{ρ} , needed in Eq. (12), can be determined by Eq. (17); see explanation in Sect. 3.5. The required value ε_{fse} has to be determined experimentally by density measurements on synthetic air, and then it can be calculated by Eq. (16) as described in Sect. 3.5.

4 Density measurements on four pure fluids and synthetic air

In order to verify the empirical correction model for the correction of the FTE, density measurements were conducted on pure methane, nitrogen, argon, and carbon dioxide. Moreover, the density of synthetic air was measured to determine the apparatus-specific constant ε_{ρ} (see Sect. 3.5). The pure gases

Table 5 Sample information

Chemical name	Source	Purity/mole fraction	Purification method
Methane	Westfalen	0.999995 ^a	None
Nitrogen	Air liquide	0.999999 ^b	None
Argon	Air liquide	0.99999 ^c	None
Carbon dioxide	Air products	0.999995 ^d	None
Ethane	GHC	0.99999 ^e	None
Helium	Air liquide	0.99999 ^f	None
Synthetic air	Air liquide	0.2094 ± 0.0020 oxygen in nitrogen ^g	None

^aImpurities (stated by supplier): $x(\text{H}_2\text{O}) \leq 2.0 \times 10^{-6}$, $x(\text{O}_2) \leq 0.5 \times 10^{-6}$, $x(\text{other } \text{C}_m\text{H}_n) \leq 0.5 \times 10^{-6}$, $x(\text{N}_2) \leq 4.0 \times 10^{-6}$, $x(\text{H}_2) \leq 0.1 \times 10^{-6}$, where x denotes mole fraction

^bImpurities (stated by supplier): $x(\text{H}_2\text{O}) \leq 0.5 \times 10^{-6}$, $x(\text{O}_2) \leq 0.1 \times 10^{-6}$, $x(\text{C}_m\text{H}_n) \leq 0.1 \times 10^{-6}$, $x(\text{CO}) \leq 0.1 \times 10^{-6}$, $x(\text{CO}_2) \leq 0.1 \times 10^{-6}$, $x(\text{H}_2) \leq 0.1 \times 10^{-6}$

^cImpurities (stated by supplier): $x(\text{H}_2\text{O}) \leq 2.0 \times 10^{-6}$, $x(\text{O}_2) \leq 2.0 \times 10^{-6}$, $x(\text{C}_m\text{H}_n) \leq 0.5 \times 10^{-6}$, $x(\text{CO}_2) \leq 0.2 \times 10^{-6}$, $x(\text{N}_2) \leq 5.0 \times 10^{-6}$

^dImpurities (stated by supplier): $x(\text{H}_2\text{O}) \leq 2.0 \times 10^{-6}$, $x(\text{O}_2) \leq 0.5 \times 10^{-6}$, $x(\text{C}_m\text{H}_n) \leq 0.1 \times 10^{-6}$, $x(\text{N}_2) \leq 2.0 \times 10^{-6}$, $x(\text{CO}) \leq 0.5 \times 10^{-6}$

^eImpurities (stated by supplier): $x(\text{H}_2\text{O}) \leq 3.0 \times 10^{-6}$, $x(\text{O}_2) \leq 1.0 \times 10^{-6}$, $x(\text{other } \text{C}_m\text{H}_n) \leq 6.0 \times 10^{-6}$, $x(\text{N}_2) \leq 3.0 \times 10^{-6}$, $x(\text{CO}/\text{CO}_2) \leq 2.0 \times 10^{-6}$

^fImpurities (stated by supplier): $x(\text{H}_2\text{O}) \leq 2.0 \times 10^{-6}$, $x(\text{O}_2) \leq 2.0 \times 10^{-6}$, $x(\text{C}_m\text{H}_n) \leq 0.2 \times 10^{-6}$, $(\text{N}_2) \leq 0.5 \times 10^{-6}$

^gImpurities (stated by supplier): $x(\text{H}_2\text{O}) \leq 2.0 \times 10^{-6}$, $x(\text{C}_m\text{H}_n) \leq 0.1 \times 10^{-6}$, $x(\text{CO}) \leq 1.0 \times 10^{-6}$, $x(\text{CO}_2) \leq 1.0 \times 10^{-6}$

and synthetic air sample are specified in Table 5; they were used as received without further gas analysis or purification.

4.1 Experimental procedure

The density measurements were carried out along isotherms. The sample gas was charged into the measuring cell with the automatic gas-dosing system. The pressures were controlled by the gas-dosing system but were measured with an independent pressure transducer as described in Sect. 2.2. An equilibration time of 60–90 min was allowed after a change in pressure, and measurements at a given pressure generally lasted 40–60 min. During a measurement run, the MSC was cycled continuously among the three weighing positions (ZP, MP1, MP2) and the balance readings, along with temperature and pressure, were recorded every 5 s. At the beginning and at the end of each isotherm, the measuring cell was evacuated in order to measure the value of $m_{S,\text{vac}}^*$ according to Eq. (6) and, moreover, to measure the zero-point offset of the pressure transducer as discussed in Sect. 2.2. These measurements were generally conducted for 30 min following an evacuation time with the turbomolecular pump of approximately 30 min. A total of four sinkers, as described

in Table 1, were used for test measurements; the results of the measurements with the Ti20a sinker in the upper position (while the SS14 sinker was in the lower position) are presented in the following Sect. 4.2 and 4.3.

4.2 Results for pure fluids

The density measurements on pure methane, nitrogen, and argon were conducted along the $T \approx 293.15$ K isotherm with pressures up to 8.0 MPa and for carbon dioxide at $T \approx 283.15$ K with pressures up to the saturation pressure. Selected results are summarized in Table 6, and comparisons with reference equations of state (EOS) for methane (Setzmann and Wagner 1991), nitrogen (Span et al. 2000), argon (Tegeler et al. 1999), and carbon dioxide (Span and Wagner 1996) are illustrated in Fig. 4. Without FTE correction, as shown in Fig. 4a, the experimental results show deviations from the reference EOS up to 1.8%. After correction of the apparatus contribution of the FTE, the deviations are much smaller and decrease to less than 0.06%. For example, the fluid-specific effect in case of methane is $\epsilon_{\text{fse}} \approx +450 \times 10^{-6}$ according to Eq. (12), with $\epsilon_\rho = 74 \times 10^{-6}$ (see Table 4). Finally, after full correction of the FTE according to Eq. (13), the bulk of the experimental results agree with the reference EOS within 0.02%, except for two values, which is a very good result for such a simple densimeter with comparatively small sinkers. One nitrogen value at $p = 2.0156$ MPa was measured at a low pressure where the uncertainty of pressure and density measurements was relatively high, and one value of carbon dioxide at $p = 4.4967$ MPa was measured very close to the vapor pressure of CO_2 (0.0052 MPa below). Repeated measurements on carbon dioxide showed that the relative deviations of the experimental densities of carbon dioxide from values calculated with the reference EOS significantly increased when the dew-point was approached. This could be attributed to adsorption and capillary condensation on the sinker surface, which made the sinker heavier, and thus the calculated density too low. The effects of such surface phenomena could be considered but this is outside the focus of the present paper and is being investigated as part of the ongoing research program of our group.

4.3 Results for synthetic air

As explained in Sect. 3.5, the apparatus-specific constant ϵ_ρ can be determined based on density measurements of synthetic air. We conducted such measurements on synthetic air (0.2094 ± 0.0020 mol fraction oxygen in nitrogen; see Table 5) using the Ti20a sinker in the top suspension position and with the SS14 sinker in the bottom position along the $T \approx 293.15$ K isotherm at pressures from (2.0 to 8.0) MPa. The results are listed in Table 3. The densities were calculated by Eq. (13) but with $\epsilon_{\text{fse}} = 0$, i.e., without correction

Table 6 Results of the density measurements on pure fluids and relative deviations $\Delta\rho/\rho = 100 \times (\rho_{\text{exp}} - \rho_{\text{EOS}})/\rho_{\text{EOS}}$ of the experimental densities ρ_{exp} from densities ρ_{EOS} calculated with reference equations of state, where T is the temperature (ITS-90) and p is the pressure

T/K	p/MPa	$\rho_{\text{EOS}}/(\text{kg m}^{-3})$	Without correction ^a		Apparatus correction only ^b		Full correction ^c		
			$\rho_{\text{exp}}/(\text{kg m}^{-3})$	$\Delta\rho/\rho$	$\rho_{\text{exp}}/(\text{kg m}^{-3})$	$\Delta\rho/\rho$	$\rho_{\text{exp}}/(\text{kg m}^{-3})$	$\Delta\rho/\rho$	
Methane									
293.196	2.0041	13.6875	13.9408	1.850	13.6949	0.054	13.6887	0.009	
293.194	3.9791	28.1889	28.4492	0.923	28.2041	0.054	28.1913	0.008	
293.194	5.9816	43.9390	44.2064	0.608	43.9622	0.053	43.9422	0.007	
293.192	7.9678	60.5335	60.8088	0.455	60.5655	0.053	60.5380	0.007	
Nitrogen									
293.186	2.0156	23.2535	23.5039	1.077	23.2514	-0.009	23.2472	-0.027	
293.189	4.0411	46.7107	46.9643	0.543	46.7131	0.005	46.7047	-0.013	
293.190	6.0583	70.0169	70.2753	0.369	70.0253	0.012	70.0127	-0.006	
293.189	8.0299	92.5963	92.8557	0.280	92.6070	0.012	92.5903	-0.007	
Argon									
293.191	2.0055	33.2994	33.5580	0.777	33.3068	0.022	33.3000	0.002	
293.197	4.0001	67.2179	67.4821	0.393	67.2329	0.022	67.2192	0.002	
293.194	5.9831	101.611	101.882	0.266	101.634	0.023	101.614	0.002	
293.192	7.9733	136.648	136.925	0.203	136.680	0.023	136.652	0.003	
Carbon dioxide									
283.172	1.9913	42.7723	42.9831	0.493	42.7816	0.022	42.7741	0.004	
283.200	4.0059	108.615	108.830	0.197	108.631	0.015	108.612	-0.003	
283.157	4.4665	132.898	133.091	0.145	132.894	-0.003	132.871	-0.021	
283.190	4.4967	134.707	134.868	0.119	134.671	-0.027	134.647	-0.045	

The presented measurements were carried out with the Ti20a sinker (see Table 1) in the top position (while the SS14 sinker was in the bottom position)

The expanded uncertainties ($k=2$) of the measurements are 16 mK for temperature, between (0.2 and 0.7) kPa for pressure, and 0.020 kg m^{-3} for density. The densities ρ_{EOS} were calculated with reference equations of state: methane (Setzmann and Wagner 1991); nitrogen (Span et al. 2000); argon (Tegeler et al. 1999); and carbon dioxide (Span and Wagner 1996)

^aTo calculate densities without FTE correction, Eq. (13) was adopted with $\epsilon_{\text{vac}}=0$ and $\epsilon_{\text{fse}}=0$ and with m_{S} instead of $m_{\text{S,vac}}^*$ (see Eq. (8))

^bEq. (13) was adopted with $\epsilon_{\text{fse}}=0$ to calculate densities with correction of the apparatus contribution $\epsilon_{\text{vac}} \approx -(57 \pm 8) \times 10^{-6}$ only

^cEq. (13) was adopted to calculate densities with full correction of the FTE

of the fluid-specific effect. The relative deviations of these experimental densities from values calculated with the GERG-2008 equation of state (Kunz and Wagner 2012) are also listed in Table 3, and they are plotted in Fig. 3. It can be seen that the relative deviations of the experimental values without the correction of the fluid-specific effect ϵ_{fse} from values calculated with the GERG-2008 equation are very large. The reason for these deviations is the large specific susceptibility of the synthetic air, $\chi_s/\chi_{s0} = 30.74$ at $T = 293.15 \text{ K}$ (see Appendix A3), which was deliberately used for these measurements. Based on the results, the apparatus-specific constant ϵ_{ρ} was determined according to Eq. (17) in Sect. 3.5.

Further measurements on synthetic air were carried out with various sinkers of different masses and materials (see Table 1) along the $T \approx 293.15 \text{ K}$ isotherm with pressures from (2.0 to 8.0) MPa. These were done to investigate the fluid-specific effect for various sinkers in different

combinations and to determine the apparatus-specific constant ϵ_{ρ} . The results are listed in Table 4.

4.4 Uncertainty analysis

The uncertainty budget for the measuring system is summarized in Table 7. As has been discussed in Sect. 2.2, the expanded uncertainty ($k=2$) in temperature and pressure measurement are 16 mK and (0.2 to 0.7) kPa, respectively. According to Eq. (13), the uncertainty in density measurement depends on the uncertainties: (1) of the weighing values $u(m_{\text{S,vac}}^*)$ and $u(m_{\text{S,fluid}}^*)$, (2) of the sinker volume $u(V_{\text{S}})$, and (3) of the FTE correction factors $u(\epsilon_{\text{vac}})$ and $u(\epsilon_{\text{fse}})$. Due to the fluctuation of the weighing values, the expanded uncertainty ($k=2$) of $m_{\text{S,vac}}^*$ and $m_{\text{S,fluid}}^*$ was estimated to be $60 \mu\text{g}$. The relative expanded uncertainty ($k=2$) of the volume of the density sinker (Ti20a) is 0.0020%.

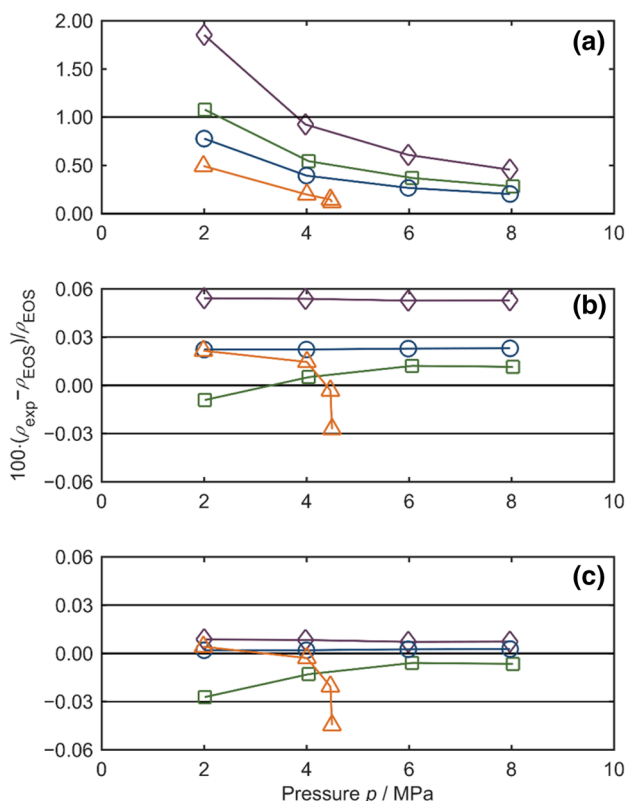


Fig. 4 Relative deviations of the experimental densities ρ_{exp} from densities ρ_{EOS} calculated with reference equations of state (see Table 6): methane (Setzmann and Wagner 1991); nitrogen (Span et al. 2000); argon (Tegeler et al. 1999); and carbon dioxide (Span and Wagner 1996). **a** Without correction of the force-transmission error (see Table 6 and Sect. 4.2); **b**: with correction of the apparatus contribution ϵ_{vac} only; **c**: with full correction according to Eq. (13). (open square), methane ($T \approx 293.15$ K); (open rhombus), nitrogen ($T \approx 293.15$ K); (open circle), argon ($T \approx 293.15$ K); (open triangle), carbon dioxide ($T \approx 283.15$ K). The presented measurements were carried out with the Ti20a sinker in the top position, while the SS14 sinker was in the bottom position

As mentioned in Sect. 3.3 and 3.5, the expanded uncertainty ($k=2$) of ϵ_{vac} was estimated to be $u(\epsilon_{\text{vac}}) = 8 \times 10^{-6}$, and the relative expanded uncertainty ($k=2$) of ϵ_{ρ} was estimated to be $u(\epsilon_{\rho})/\epsilon_{\rho} = 6\%$. According to Eq. (12), the relative expanded uncertainty ($k=2$) of ϵ_{fse} was estimated to be $u(\epsilon_{\text{fse}})/\epsilon_{\text{fse}} = 10\%$ (see Sect. 3.5). Thus, the relative standard uncertainty of the density measurement can now be determined according to the ‘‘Guide to the Expression of Uncertainty in Measurement’’ (ISO/IEC Guide 98-3 2008; GUM 1995):

$$\frac{u(\rho_{\text{fluid}})}{\rho_{\text{fluid}}} = \left[\frac{u(m_{\text{S,vac}}^*)^2 + u(m_{\text{S,fluid}}^*)^2}{(m_{\text{S,vac}}^* - m_{\text{S,fluid}}^*)^2} + \left(\frac{u(V_{\text{S}})}{V_{\text{S}}} \right)^2 + \frac{u(\epsilon_{\text{vac}})^2 + u(\epsilon_{\text{fse}})^2}{(1 + \epsilon_{\text{vac}} + \epsilon_{\text{fse}})^2} \right]^{0.5}, \tag{18}$$

and the minimum (absolute) standard uncertainty can be calculated by:

$$u(\rho_{\text{fluid}}) = \left[u(m_{\text{S,vac}}^*)^2 + u(m_{\text{S,fluid}}^*)^2 \right]^{0.5} \times V_{\text{S}}^{-1}, \tag{19}$$

As a result, the expanded uncertainty ($k=2$) in density was estimated to be $0.020 \text{ kg}\cdot\text{m}^{-3}$ (see Table 7). The denominator $(1 + \epsilon_{\text{vac}} + \epsilon_{\text{fse}})$ in the last term of Eq. (19) has already been set to 1.0; the influence of this simplification on the result is negligibly small. The combined expanded uncertainty ($k=2$) of the fluid density, including the uncertainties in temperature and pressure can now be estimated by:

$$u_{\text{C}}(\rho) = \left[u(\rho)^2 + \left(\left(\frac{\partial \rho}{\partial T} \right)_p \times u(T) \right)^2 + \left(\left(\frac{\partial \rho}{\partial p} \right)_T \times u(p) \right)^2 \right]^{0.5}, \tag{20}$$

where the partial derivatives (sensitivity coefficients) can be calculated with the reference equations of state for the respective fluid (see above). In case of synthetic air, the influence of the uncertainty of the composition $u(\rho(x)) = (\Delta\rho/\Delta x_{\text{O}_2}) \cdot u(x_{\text{O}_2})$ was also considered in Eq. (20). The combined expanded uncertainty ($k=2$) of the fluid density for a selected example is given in Table 7 as 0.0319%. It can be seen in the table that the major contributions to this uncertainty (after correction of the FTE) are the uncertainty of temperature, pressure, and weighing values.

5 Sorption measurements

As a typical example, the adsorption of carbon dioxide on zeolite 13X was measured at $T \approx 283.15$ K, with the zeolite in a small sample container. The container is cup-shaped (outer diameter: 16 mm, wall thickness: 0.5 mm, height: 20 mm, material: stainless steel) with a hanger on top. The container with the zeolite was in the lower suspension position of the gravimetric sorption analyzer, and the Ti20a sinker was in the upper position to measure the density of the sample gas. The mass and the volume of the container are $m_{\text{C}} \approx 2.4$ g and $V_{\text{C}} \approx 0.30 \text{ cm}^3$, and of zeolite $m_{\text{Z}} \approx 2.2$ g and $V_{\text{Z}} \approx 0.34 \text{ cm}^3$. As a second typical example, the adsorption of carbon dioxide on the surface of the density sinker Ti20a and on the surface of the sorption sinker SS09 were also measured. The results of these

Table 7 Uncertainty budget for density measurements

Source	Uncertainty U ($k=2$)	Contribution to $U(\rho)/\rho$ ($k=2$)
Temperature T	16 mK	0.0200%
Pressure p	0.4 kPa	0.0168%
Weighing value $m_{S,vac}^*$ ^a	60 μg	0.0127%
Weighing value $m_{S,fluid}^*$ ^a	60 μg	0.0127%
Sinker volume $V_S(T,p)$	0.0020%	0.0020%
FTE correction factors		
Apparatus contribution ε_{vac} (-53×10^{-6})	8.0×10^{-6}	0.0008%
Apparatus-specific constant ε_p (76×10^{-6})	5×10^{-6}	
Fluid-specific effect ε_{fse} (201×10^{-6})	20×10^{-6}	0.0020%
Density ρ	0.020 kg m^{-3}	
Relative combined expanded uncertainty ($k=2$) in density $U_C(\rho)/\rho$		0.0319%

As an example, the measurement on carbon dioxide at ($T=283.195$ K, $p=4.0026$ MPa, $\rho=108.612$ kg m^{-3}) was taken. The Ti20a sinker (see Table 1) was in the top position to measure the density. (The sinker SS09 was in the bottom position)

^aDifference value ($m_{S,vac}^* - m_{S,fluid}^*$) = 0.472805 g

investigations and a detailed uncertainty analysis will be presented in a companion paper (Yang et al. 2019). Furthermore, the adsorption on the surface of four different sinkers and on zeolite were recently measured in the vicinity of the dew point of carbon dioxide, ethane and one gas mixture. The results of these investigations will be presented by Yang and Richter (2019).

Since the absorption on the porous zeolite sample is relatively large and the volume of the zeolite sample is relatively small, the influence of the FTE correction factors ε_{vac} and ε_{fluid} on the result, the absorbed mass m_{sorp} , is very small and can usually be neglected. Furthermore, in such cases, the influence of the uncertainty of the sample-fluid density is also negligibly small. In the special case of accurate investigations of adsorption on less-porous adsorbents and solid metal surfaces, however, the adsorption on the surface of the “sorption sinker” (e.g., our Ti20a sinker, see Table 1) is relatively small and the volume of the sinker is relatively large. Then, the influence of the FTE correction factors ε_{vac} and ε_{fluid} on the result m_{sorp} can be significant, and the influence of the uncertainty of the sample-fluid density on m_{sorp} should be considered. The magnitude of these uncertainties will also be presented and discussed in a companion paper (Yang et al. 2019).

6 Conclusions

The FTE of a gravimetric sorption analyzer, which incorporates a MSC as a key component, was systematically investigated. For this investigation, the instrument was equipped with a second density sinker instead of the usual

sample container for a porous material and, thus, it was used as “tandem-sinker densimeter”. To correct the FTE and to achieve a lower uncertainty of the sorption analyzer, an empirical solution was derived to calculate the fluid density based on one sinker, and to calculate the adsorbed mass on another sinker, which could also be a small sample container filled with sample of porous material. The FTE can be separated into two parts: (1) an apparatus contribution and (2) a fluid contribution. The characteristic of the apparatus contribution to the FTE was investigated by measurements in vacuum. The results showed that the apparatus contribution to the FTE increased with increasing suspended load on the MSC. The fluid contribution of the FTE is proportional to the density of the sinker, minus the fluid density, and to the specific magnetic susceptibility of the sample fluid; the proportionality factor is an apparatus-specific constant that can be determined by density measurements of synthetic air. For the correction of the FTE, an empirical correction model was developed. This model can equally be applied to single-sinker densimeters. The expanded uncertainty ($k=2$) of the measuring system used was estimated to be: 16 mK for temperature, (0.2–0.7) kPa for pressure, 0.020 kg m^{-3} in density.

The empirical correction model was successfully verified by comparing the measurement results of four pure fluids (methane, nitrogen, argon, and carbon dioxide) with the corresponding reference equations of state. As adsorption examples, the adsorption of carbon dioxide on zeolite 13X and on non-porous material were measured at $T \approx 283.15$ K; these results are presented in a companion paper (Yang et al. 2019). We note that in order to obtain accurate results, it is important to correct the FTE caused by the MSC. When the best achievable accuracy is not necessary, a few correction

terms can be omitted (see Sect. 3.2). For oxygen-containing gas mixtures, however, this should be carefully considered.

Acknowledgements The authors are grateful to Deutsche Forschungsgemeinschaft (DFG) for funding their on-going research on new approaches for measurement and modelling of fluid mixture dew-point densities within the Emmy Noether Programme under Grant No. RI 2482/2-1.

Appendix A

A1 Additional information to Sect. 3

Annotation 1 (to Sect. 3.1)

For most applications Eq. (13) can be slightly simplified. Since $|\epsilon_{vac}| \ll 1$ and $|\epsilon_{fse}| \ll 1$, the value $1/(1 + \epsilon_{vac} + \epsilon_{fse})$ in Eq. (13) can be replaced by:

$$1/(1 + \epsilon_{vac} + \epsilon_{fse}) \approx (1 - \epsilon_{vac} - \epsilon_{fse}), \tag{21}$$

which yields:

$$\rho_{fluid} = \frac{m_{S,vac}^* - m_{S,fluid}^*}{V_S} \times (1 - \epsilon_{vac} - \epsilon_{fse}). \tag{22}$$

For diamagnetic fluids and fluid mixtures, the value ϵ_{fse} is usually less than 1000×10^{-6} and, therefore, the influence of the simplification on the density ρ_{fluid} is usually negligibly small (less than 1×10^{-6}). The value ϵ_{vac} , which does not depend on the sample fluid, is also very small (less than 60×10^{-6} ; see Table 2). For paramagnetic fluids and fluid mixtures, the value ϵ_{fse} is in most cases less than 3000×10^{-6} (e.g. for oxygen-containing fluid mixtures with mole fractions of oxygen up to 0.06), and the influence of the simplification is less than 9×10^{-6} . For air with a mole fraction of oxygen of about 0.21, however, the value ϵ_{fse} is approximately 0.01 and the influence of the simplification would be approximately 100×10^{-6} . Therefore, for $\epsilon_{fse} \geq 3000 \times 10^{-6}$, Eq. (13) should be used instead of Eq. (22).

Annotation 2 (to Sect. 3.2)

The error in density of the sample fluid $\Delta\rho_{FTE}$ due to the force-transmission error of the magnetic-suspension coupling can be determined as: $\Delta\rho_{FTE} = (\rho_{fluid,uncorr} - \rho_{fluid})$. Both densities ρ_{fluid} and $\rho_{fluid,uncorr}$ have to be determined using Eq. (13) or (22); in the case of $\rho_{fluid,uncorr}$ the value $m_{S,vac}^*$ has to be replaced by $m_S \cdot (1 + \epsilon_{vac})$ according to Eq. (8), and the two FTE correction terms have to be set to zero, i.e., $\epsilon_{vac} = 0$ and $\epsilon_{fse} = 0$. Then, the error in density $\Delta\rho_{FTE}$, in the case where the force-transmission error is not corrected, can be calculated with the derived equation:

$$\Delta\rho_{FTE} = \epsilon_{vac} \times [\rho_{fluid} - \rho_S \times (1 + \epsilon_{vac})] + \epsilon_{fluid} \times (\rho_{fluid} - \rho_S). \tag{23}$$

The values ϵ_{vac} and ϵ_{fse} can be determined with Eqs. (15) and (12), respectively. The term $(1 + \epsilon_{vac})$ in Eq. (23) can be omitted because its influence on the value $\Delta\rho_{FTE}$ is negligibly small (less than 1×10^{-6}). Then, the result is a simple equation:

$$\Delta\rho_{FTE} = \epsilon_{vac} \times (\rho_{fluid} - \rho_S) + \epsilon_{fluid} \times (\rho_{fluid} - \rho_S). \tag{24}$$

The same result has already been derived by McLinden et al. (2007), and it has been presented in their paper as Eq. (25). In order to clearly demonstrate the reason for the force-transmission error, Eq. (24) can be multiplied by the volume V_S of the sinker and with $\rho_S \times V_S = m_S$; this yields:

$$\Delta\rho_{FTE} \cdot V_S = -(\epsilon_{vac} + \epsilon_{fluid}) \times (m_S - \rho_{fluid} \cdot V_S), \tag{25}$$

where $\Delta\rho_{FTE} \times V_S = \Delta m_{FTE}$ corresponds to the FTE in mass units. This result is given in Sect. 3.2 as Eq. (14). (Please note that for two-sinker densimeters (see Sect. 1), the term ρ_S does not exist in Eq. (24) and the term m_S does not exist in Eq. (25). This is because in a two-sinker densimeter both sinkers are nominally of the same mass and they were changed on the sinker support, thus, both sinkers were weighed with nearly the same position of the permanent magnet.)

Annotation 3 (to Sect. 3.4)

The magnitude of the apparatus contribution ϵ_{vac} of the FTE depends on the magnetic properties of the material of the coupling housing and the components in its vicinity. The magnetic properties of metals and fluids are characterized by their magnetic susceptibility χ . For example, copper, beryllium, and zirconium are diamagnetic metals and their specific magnetic susceptibilities (negative values) are $\chi_s/\chi_{s0} = -0.11, -1.26,$ and $-1.65,$ respectively, where $\chi_{s0} = 10^{-8} \text{ m}^3 \text{ kg}^{-1}$ is a reducing constant (CRC Handbook 2016). Alloys of these metals (plus chromium) are commonly used for coupling housings, e.g., CuBe2 and CuCr1Zr with $\chi_s/\chi_{s0} = -0.018$ and $-0.025,$ respectively. Paramagnetic metals, for example, are chromium and manganese with $\chi_s/\chi_{s0} = +4.0$ and $+11.7,$ respectively, at $T \approx 293.15 \text{ K}$ (CRC Handbook 2016); but nickel, for example, is a ferromagnetic material, and stainless steels can be paramagnetic or ferromagnetic. The susceptibility of diamagnetic substances varies only slightly with temperature (or not at all); in contrast, paramagnetic substances show a much stronger temperature dependence, varying roughly as $1/T$ (CRC Handbook 2016).

The values ϵ_{vac} are positive for diamagnetic coupling housings and negative for paramagnetic coupling housings. However, elements of paramagnetic metals in the vicinity of

diamagnetic coupling housings can change their magnetic properties from diamagnetic to paramagnetic. The susceptibility of diamagnetic substances varies only slightly with temperature; in contrast to that, paramagnetic substances show a much stronger temperature dependence, varying roughly as $1/T$ (CRC Handbook 2016). For example, the measuring cell of the two-sinker densimeter at NIST was made of a (diamagnetic) beryllium copper alloy and the value ε_{vac} was determined to be $(15.3 \pm 1.8) \times 10^{-6}$ (McLinden et al. 2007); it is approximately constant over the temperature range of (265–500) K. However, elements of paramagnetic metals in the vicinity of diamagnetic coupling housings can change their magnetic properties from diamagnetic to paramagnetic. As a revealing example, the measuring cell of our group's single-sinker densimeter for cryogenic temperatures (Richter et al. 2016) was also made of a (diamagnetic) beryllium copper alloy (CuBe2). However, in the vicinity of the magnetic-suspension coupling, several parts made of the material Inconel 600 were inadvertently installed instead of Inconel 625, and Inconel 600 becomes strongly paramagnetic at very low temperatures. As a result, the values ε_{vac} ranged from -7×10^{-6} at $T = 293.15$ K to -366×10^{-6} at $T = 105$ K (Richter et al. 2016). After replacing the parts made of Inconel 600 with new ones made of Inconel 625, the magnetic susceptibility of the measuring cell changed from paramagnetic to diamagnetic, and the values ε_{vac} ranged from $+19 \times 10^{-6}$ at $T = 298.15$ K to $+12 \times 10^{-6}$ at $T = 100$ K (Lentner et al. 2017), which are typical values.

The coupling housing of the apparatus used in the present work is made of a diamagnetic CuBe2 alloy. However, the negative characteristic values ε_{vac} (see Table 2) of the coupling housing show that its magnetic properties are paramagnetic. Since there are no paramagnetic or ferromagnetic parts in the vicinity of the coupling housing, we assume that there are ferromagnetic particles in the separating wall of the coupling housing above the permanent magnet. This can happen when small ferromagnetic particles inadvertently get into the measuring cell together with the porous sample or the sample gas and then accumulate on the permanent magnet. Due to incorrect operation of the magnetic-suspension coupling, the permanent magnet may occasionally bounce against the separating wall and push the ferromagnetic particles into the disc. The coupling housing of the sorption analyzer we currently use was manufactured in 2010, and since then the analyzer has been used by several groups of our institute for various applications. Therefore, we could not find out what happened with the coupling housing. A small temperature dependence of the value ε_{vac} was ascertained; it changed from approximately -55×10^{-6} at $T \approx 293.15$ K to -51×10^{-6} at $T \approx 323.15$ K, which is within the uncertainty of the value ε_{vac} (8×10^{-6}).

Annotation 4 (to Sect. 3.5)

The FTE correction model and the term ε_{fse} can also be used for oxygen-containing mixtures with oxygen mole fractions up to about 0.20. For example, the presented measurements on the synthetic air sample (see Table 3) can also be corrected with this model. For the Ti20a sinker in the top position, the current relative deviations $(\rho_{\text{exp,uncorr}} - \rho_{\text{GERG}})/\rho_{\text{GERG}}$ of the first four density measurements at $\rho_{\text{exp,uncorr}} = (23.5112, 47.1581, 71.2443$ and $94.7417) \text{ kg m}^{-3}$ are $(-1.027, -0.999, -0.980$ and $-0.959)\%$, respectively; see Table 3. After correction, these deviations decreased to only $(0.020, 0.043, 0.056$ and $0.072)\%$, respectively. Since the constant ε_{ρ} was determined by extrapolating the density deviation to $\rho_{\text{fluid}} = 0$, the reason for these residual deviations are the uncertainty of the measurements on the synthetic air sample and the uncertainty of the GERG equation, or more precisely, the slope of the values calculated with this equation in the gas region.

With regard to the possible temperature dependence of the apparatus-specific constant ε_{ρ} , some experimental experience can be reported. For diamagnetic coupling housings, the apparatus-specific constant ε_{ρ} depends only slightly on temperature (or not at all); e.g., for the two-sinker densimeter at NIST (McLinden et al. 2007), the value $\varepsilon_{\rho} = 51.7 \times 10^{-6}$ remains approximately constant (for six diamagnetic fluids and air) in the temperature range from (250 to 500) K. For strong paramagnetic coupling housings, however, where the magnetic properties and the characteristic value ε_{vac} may change significantly with temperature, the value ε_{ρ} may also change with temperature. At the end of the second paragraph in Appendix A1, Annotation 3, we mentioned our group's low-temperature single-sinker densimeter, where the magnetic properties of the coupling housing and its characteristic value ε_{vac} increased significantly from -7×10^{-6} at $T = 293.15$ K to -366×10^{-6} at $T = 105$ K due to unfavorable material in the vicinity of the magnetic-suspension coupling. It is possible that the value $\varepsilon_{\rho} = (50 \pm 10) \times 10^{-6}$ at that time was also influenced by this fact and increased. As a result, the correction of the existing fluid-specific effect would not have been sufficient and, as ascertained, a residual error in the test density measurement on methane of 0.017% at $T = 105$ K could occur (see Richter et al. 2016, Section 4.1 and Fig. 6). A replacement of the apparatus-specific constant from the fixed value of $\varepsilon_{\rho} = 50 \times 10^{-6}$ to a temperature-dependent parameter $\varepsilon_{\rho}(T) = (50 \text{ to } 116) \times 10^{-6}$ for the temperature range from (293.15 to 105) K would eliminate this residual error. At present, this is an assumption, which should only be considered if necessary. After replacing the wrong paramagnetic parts made of Inconel 600 with diamagnetic ones made of Inconel 625 (see Appendix A1, Annotation 3), the susceptibility of the measuring cell changed from paramagnetic to diamagnetic and the newly determined

apparatus-specific constant $\epsilon_\rho = (54 \pm 5) \times 10^{-6}$ was approximately constant over the temperature range from (293.15 to 100) K (Lentner et al. 2018; Eckmann et al. 2018).

Annotation 5 (to Sect. 3.5)

For the determination of the apparatus-specific constant ϵ_ρ according to Eq. (17), the density ρ_s of the sinker is needed. In case of a container filled with a porous sample, this “density ρ_s ” can be estimated by the mass $m_{CP} = (m_C + m_P)$ and the volume $V_{CP} = (V_C + V_P)$ of the container (C) with the porous sample (P) to be: $\rho_{CP} = m_{CP}/V_{CP}$. The required value ϵ_{fse} of the fluid-specific effect in Eq. (17) can be determined by Eq. (16) on the basis of density measurements in synthetic air. As a suitable alternative, instead of the porous sample in the container, a solid metal piece (or pieces of metal, glass or suitable plastic) with approximately the same mass m_P can be used or, as a second alternative, a solid metal sinker with approximately the same total mass m_{CP} can be used. It can be seen in Table 4 that the apparatus-specific constant ϵ_ρ for sinkers in the bottom position is approximately independent of the mass and the density of the sinker. However, for the determination of the fluid-specific effect ϵ_{fse} according to Eq. (12) for subsequent measurements with the sample-filled container in a sample gas, an estimated value of the density ρ_{CP} has to be used.

A2 Susceptibility of pure gases and gas mixtures

The magnetic molar susceptibility χ_{mol} of gas mixtures can be calculated by the following equation (Davis 1998):

$$\chi_{mol} = \sum_i x_i \times \chi_{mol,i}, \tag{26}$$

where x_i is the mole fraction of a component i in a gas mixture and $\chi_{mol,i}$ is the molar susceptibility of this component. With $\chi_{mol} = \chi_s \times M$, the specific magnetic susceptibility χ_s of a gas mixture can be determined:

$$\chi_s = \sum_i x_i \times (M_i/M) \times \chi_{s,i}, \tag{27}$$

where M_i is the molar mass of a component i in a gas mixture, M is the molar mass of the gas mixture, with $M = \sum_i (x_i \times M_i)$, and $\chi_{s,i}$ is the specific susceptibility of a component i .

The magnetic susceptibility of most common pure fluids is diamagnetic, e.g., methane, ethane, propane, nitrogen, argon, carbon dioxide, hydrogen, and helium with specific susceptibilities (negative values) at $T \approx 293.15$ K of $\chi_s/\chi_{s0} = -1.36, -1.12, -1.10, -0.54, -0.61, -0.60, -2.49,$ and $-0.63,$ respectively, where $\chi_{s0} = 10^{-8} \text{ m}^3 \times \text{kg}^{-1}$ is a reducing constant (CRC Handbook 2016). The susceptibility of diamagnetic fluids varies only slightly with temperature (CRC Handbook

2016). The standard uncertainty of these values were estimated by us to be 2%.

In contrast to diamagnetic fluids, the susceptibility of paramagnetic fluids is much greater and show a much stronger temperature dependence, varying roughly as $1/T$ (CRC Handbook 2016). The most important paramagnetic fluids are oxygen and oxygen-containing mixtures, in particular air. The specific susceptibility of oxygen and synthetic air is given in Appendix A3.

Note that we use specific magnetic susceptibilities, χ_s , in SI units ($\text{m}^3 \text{ kg}^{-1}$); values in the old cgs system ($\text{cm}^3 \text{ mol}^{-1}$) are often encountered in handbooks, including in the CRC Handbook. The conversion between the two systems is given by $\chi_s/(10^{-9} \text{ m}^3 \text{ kg}^{-1}) = [\chi_{mol}/(10^{-6} \text{ cm}^3 \text{ mol}^{-1})] \times 4\pi \times [(1/M) \times (\text{g/mol})]$, where χ_{mol} is the molar magnetic susceptibility (in the cgs system) and M is the molar mass of the substance.

A3 Susceptibility of oxygen and synthetic air

The specific susceptibility of (paramagnetic) oxygen is very large and depends strongly on temperature:

$$\chi_{s,O_2}(T) = (1341.3 \times 10^{-9} \text{ m}^3 \times \text{kg}^{-1}) \times (293.15 \text{ K}/T) \tag{28}$$

where the first value is the specific susceptibility of oxygen at $T = 293.15$ K (May et al. 2008), and its temperature dependence is $(293.15 \text{ K}/T)$ (Davis 1998). We estimate the standard uncertainty of the value $\chi_{s,O_2}(T)$, to be 2%. A previous value of the specific susceptibility of oxygen at $T = 293.15$ K was given by Davis (1998): $\chi_{s,O_2} = +1340.0 \times 10^{-9} \text{ m}^3 \text{ kg}^{-1}$ (standard uncertainty 1%); the new value, $\chi_{s,O_2} = +(1341.3 \pm 1.9) \times 10^{-9} \text{ m}^3 \text{ kg}^{-1}$, measured by May et al. (2008), is approximately 0.10% higher and its uncertainty is much less.

The specific susceptibility of synthetic air can be calculated with Eq. (27) as:

$$\chi_{s,air}(T) = x_{O_2} \times (M_{O_2}/M_{air}) \times \chi_{s,O_2}(T) + x_{N_2} \times (M_{N_2}/M_{air}) \times \chi_{s,N_2} \tag{29}$$

where x_{O_2} and x_{N_2} are the mole fractions of the components, M_{air} is the molar mass of synthetic air, with $M_{air} = (x_{O_2} \times M_{O_2} + x_{N_2} \times M_{N_2})$, $\chi_{s,O_2}(T)$ is the temperature dependent specific susceptibility of oxygen, according to Eq. (28), and $\chi_{s,N_2} = -5.38 \times 10^{-9} \text{ m}^3 \text{ kg}^{-1}$ at $T = 293.15$ K is the specific susceptibility of nitrogen, that is only slightly temperature-dependent (or not at all) (CRC Handbook 2016). Hence, the specific susceptibility of our synthetic air sample (0.2094 mol fraction oxygen in nitrogen) is $\chi_{s,air} = +307.4 \times 10^{-9} \text{ m}^3 \text{ kg}^{-1}$ at $T = 293.15$ K, with $M_{O_2} = 32.00 \text{ g mol}^{-1}$, $M_{N_2} = 28.01 \text{ g mol}^{-1}$, and $M_{air} = 28.85 \text{ g mol}^{-1}$.

It should be mentioned here that the specific susceptibility of oxygen also depends on the density ρ_{O_2} of oxygen (Perrier and Kamerlingh Onnes 1914; Woltjer et al. 1929; May

et al. 2008). Based on the experimental results of Woltjer et al. (1929), we estimated that the specific susceptibility of oxygen, $\chi_{s,O_2}(T)$, decreases by approximately $-2.1\% \times (\rho_{O_2}/100 \text{ kg m}^{-3})$. Therefore, the specific susceptibility of air also depends on density. Since the influence of the specific susceptibility of nitrogen on that of air is relatively small (approximately 1.3%, see Eq. (29)), the specific susceptibility of our synthetic air sample, $\chi_{s,air}(T)$, also decreases by approximately $-2.13\% \times (\rho_{air}/100 \text{ kg m}^{-3})$, where ρ_{air} is the air density. However, the influence of this change of $\chi_{s,air}$ on the determination of the apparatus-specific constant ε_ρ according to Eq. (17) is usually less than 1% because the air densities, ρ_{air} , measured in the gas region, are typically small (see explanations in Sect. 3.5). Therefore, this influence can be neglected because it is much smaller than the uncertainty of the apparatus-specific constant ε_ρ .

A4 Volume of a titanium sinker as function of temperature and pressure

For a silicon sinker, the volume change with temperature and pressure was described in detail by Richter et al. (2016) in their Appendices A2 and A3. For a titanium sinker, the sinker volume at different temperatures and pressures can be calculated by:

$$V_S(T, p) = V_{S0} \times \left[1 + 3 \times \overline{\alpha_L}|_{T_0}^T \times (T - T_0) - \frac{1}{K(T)} \times (p - p_0) \right], \quad (30)$$

where V_{S0} is the volume of the sinker at reference conditions (here, $T_0 = 293.15 \text{ K}$, $p_0 = 0.101325 \text{ MPa}$), $\overline{\alpha_L}|_{T_0}^T$ is the average linear thermal expansion coefficient in the temperature range from T_0 to T , and $K(T)$ is the bulk modulus. With the definition:

$$\varepsilon_L(T) = \overline{\alpha_L}|_{T_0}^T \times (T - T_0) \quad (31)$$

inserted in Eq. (30) gives:

$$V_S(T, p) = V_{S0} \times \left[1 + 3 \times \varepsilon_L(T) - \frac{1}{K(T)} \times (p - p_0) \right], \quad (32)$$

where $\varepsilon_L(T)$ is the length change of a solid body in the temperature range from $T_0 = 293.15 \text{ K}$ to T which can be calculated by:

$$\varepsilon_L(T) = \left(-0.1980 + 0.5072 \times \tau + 0.6500 \times \tau^2 - 0.2203 \times \tau^3 \right) \times 10^{-2}, \quad (33)$$

where $\tau = (T/1000 \text{ K})$ is a reduced temperature. Equation (33) is valid in the temperature range from (150 to 1156) K, and its uncertainty was given to be 3% (Touloukian et al. 1975). For example, at $T = 400 \text{ K}$ the equation yields $\varepsilon_L = 0.0948\%$.

The bulk modulus of titanium is $K(T_0) = 115.5 \times 10^3 \text{ MPa}$ at $T_0 = 293.15 \text{ K}$; this value was calculated with the elastic moduli C_{11} and C_{12} given by Fisher and Renken (1964); the calculation equation is explained by Richter et al. (2016) in Appendix A3. The temperature dependence of the elastic moduli is also described by Fisher and Renken, and using these values, the bulk modulus in the temperature range from (273.15 to 523.15) K can be described as:

$$K(T) = (115.5 \times 10^3 \text{ MPa}) \times \left[1 - 0.0070 \times (T - T_0)/100 \text{ K} \right] \quad (34)$$

The standard uncertainty of the bulk modulus in this temperature range was estimated by us to be 0.25%.

References

- Brachthäuser, K., Kleinrahm, R., Lösch, H.-W., Wagner, W.: Entwicklung eines neuen Dichtemessverfahrens und Aufbau einer Hochtemperatur-Hochdruck-Dichtemessanlage. Fortschr.-Ber. VDI, Reihe 8, Nr. 371. VDI-Verlag, Düsseldorf (1993)
- Cavenati, S., Grande, C.A., Rodrigues, A.E.: Adsorption equilibrium of methane, carbon dioxide, and nitrogen on zeolite 13X at high pressures. J. Chem. Eng. Data **49**, 1095–1101 (2004)
- Clark, J.W.: An electronic analytical balance. Rev. Sci. Instrum. **18**, 915–918 (1947)
- Cristancho, D.E., Mantilla, I.D., Ejaz, S., Hall, K.R., Iglesias-Silva, G.A., Atilhan, M.: Force transmission error analysis for a high-pressure single-sinker magnetic suspension densimeter. Int. J. Thermophys. **31**, 698–709 (2010)
- Davis, R.: Equation for the volume magnetic susceptibility of moist air. Metrologia **35**, 49–55 (1998)
- Dreisbach, F., Lösch, H.W.: Magnetic suspension balance for simultaneous measurement of a sample and the density of the measuring fluid. J. Therm. Anal. Calorim. **62**, 515–521 (2000)
- Eckmann, P., Kleinrahm, R., Span, R., Richter, M.: Comparison of experimental densities of synthetic air with values predicted by molecular simulation in the temperature range from (100 to 298) K at pressures up to 8 MPa. Poster, 20th Symposium on Thermophysical Properties, Boulder, USA: (2018)
- Fisher, E.S., Renken, C.J.: Single-crystal elastic moduli and the hcp \rightarrow bcc transformation in Ti, Zr, and Hf. Phys. Rev. **135**, A482–A494 (1964)
- Gast, Th: Microweighing in vacuo with a magnetic suspension balance. In: Behrndt, K.H. (ed.) Vacuum Microbalance Techniques, vol. 3, pp. 45–54. Plenum Press, New York (1963)
- Gast, Th: Entwicklung und Anwendung Elektrischer Methoden zur Registrierenden Mikrowägung. Acta Imeko **4**, 159–171 (1967)
- Gast, Th: Waagen mit freischwebender magnetischer Aufhängung. Naturwissenschaften **56**, 434–438 (1969)
- Haynes, W.M., Lide, D.R., Bruno, T.J. CRC Handbook of Chemistry and Physics, 97th edn. (eds.), CRC press, Boca Raton (2016)
- Hefti, M., Marx, D., Joss, L., Mazzotti, M.: Adsorption equilibrium of binary mixtures of carbon dioxide and nitrogen on zeolites ZSM-5 and 13X. Microporous Mesoporous Mater. **215**, 215–228 (2015)
- ISO/IEC Guide 98-3: Uncertainty of measurement—part 3: guide to the expression of uncertainty in measurement (GUM:1995). International Organization for Standardization, Geneva (2008)
- Kano, Y., Kayukawa, Y., Fujii, K., Sato, H.: A new method for correcting a force transmission error due to magnetic effects

- in a magnetic levitation densimeter. *Meas. Sci. Technol.* **18**, 659–666 (2007)
- Kayukawa, Y., Kano, Y., Fujii, K., Sato, H.: Absolute density measurements by dual sinker magnetic levitation densimeter. *Metrologia* **49**, 513–521 (2012)
- Kleinrahm, R., Wagner, W.: Entwicklung und Aufbau einer Dichtemesanlange zur Messung der Siede- und Taudichten reiner fluider Stoffe auf der gesamten Phasengrenzkurve. *Fortschr.-Ber. VDI, Reihe 3, Nr. 92*. VDI-Verlag, Düsseldorf (1984)
- Kleinrahm, R., Wagner, W.: Measurement and correlation of the equilibrium liquid and vapour densities and the vapour pressure along the coexistence curve of methane. *J. Chem. Thermodyn.* **18**, 739–760 (1986)
- Klimeck, R.: Weiterentwicklung einer Ein-Senkörper-Dichtemesanlange und Präzisionsmessungen der thermischen Zustandsgrößen von Kohlendioxid, Argon, Stickstoff und Methan. Dissertation, Ruhr-Universität Bochum, Bochum: (1997)
- Klimeck, R., Kleinrahm, R., Wagner, W.: An accurate single-sinker densimeter and measurements of the (p , ρ , T) relation of argon and nitrogen in the temperature range from (235 to 520) K at pressures up to 30 MPa. *J. Chem. Thermodyn.* **30**, 1571–1588 (1998)
- Kunz, O., Wagner, W.: The GERG-2008 wide-range equation of state for natural gases and other mixtures: an expansion of GERG-2004. *J. Chem. Eng. Data* **57**, 3032–3091 (2012)
- Kuramoto, N., Fujii, K., Waseda, A.: Accurate density measurements of reference liquids by a magnetic suspension balance. *Metrologia* **41**, S84–S94 (2004)
- Lentner, R., Richter, M., Kleinrahm, R., Span, R.: Density measurements of liquefied natural gas (LNG) over the temperature range from (105 to 135) K at pressures up to 8.9 MPa. *J. Chem. Thermodyn.* **112**, 68–76 (2017)
- Lentner, R., Kleinrahm, R., Eckmann, P., Span, R., Richter, M.: Density measurements of five methane-rich mixtures over the temperature range from (100 to 180) K at pressures up to 9.7 MPa. *J. Chem. Thermodyn.* (2019)
- Lösch, H.W.: Entwicklung und Aufbau von neuen Magnetschwebwaagen zur berührungsfreien Messung vertikaler Kräfte. *Fortschr.-Ber. VDI, Reihe 3, Nr. 138*. VDI-Verlag, Düsseldorf (1987)
- Lösch, H.W., Kleinrahm, R., Wagner, W.: Neue Magnetschwebwaagen für gravimetrische Messungen in der Verfahrenstechnik. *Chem. Ing. Tech.* **66**, 1055–1058 (1994a)
- Lösch, H.W., Kleinrahm, R., Wagner, W.: Jahrbuch 1994: Verfahrenstechnik und Chemieingenieurwesen, pp. 117–137. VDI-Verlag, Düsseldorf (1994b)
- May, E.F., Miller, R.C., Shan, Z.: Densities and dew points of vapor mixtures of (methane + propane) and (methane + propane + hexane) using a dual-sinker densimeter. *J. Chem. Eng. Data* **46**, 1160–1166 (2001)
- May, E.F., Moldover, M.R., Schmidt, J.W.: Electric and magnetic susceptibilities of gaseous oxygen: present data and modern theory compared. *Phys. Rev. A* **78**, 032522 (2008)
- McLinden, M.O.: Experimental Techniques I: Direct Methods. In: Wilhelm, E., Letcher, T.M. (eds.) *Volume properties: liquids, solutions and vapours*, pp. 73–99. The Royal Society of Chemistry, Cambridge (2015)
- McLinden, M.O., Kleinrahm, R., Wagner, W.: Force transmission errors in magnetic suspension densimeters. *Int. J. Thermophys.* **28**, 429–448 (2007)
- Moritz, K., Kleinrahm, R., McLinden, M.O., Richter, M.: Development of a new densimeter for the combined investigation of dew-point densities and sorption phenomena of fluid mixtures. *Meas. Sci. Technol.* **28**, 127004 (5 pp.) (2017)
- Perrier, A., Kamerlingh Onnes, H.: *Magnetic Investigations. XIII. The Susceptibility of Liquid Mixtures of Oxygen and Nitrogen, and the Influence of Mutual Distance of the Molecules Upon Paramagnetism*, pp. 37–54. Springer, Dordrecht, (1914)
- Richter, M., Kleinrahm, R., Lentner, R., Span, R.: Development of a special single-sinker densimeter for cryogenic liquid mixtures and first results for a liquefied natural gas (LNG). *J. Chem. Thermodyn.* **93**, 205–221 (2016)
- Setzmann, U., Wagner, W.: A new equation of state and tables of thermodynamic properties for methane covering the range from the melting line to 625 K at pressures up to 1000 MPa. *J. Phys. Chem. Ref. Data* **20**, 1061–1155 (1991)
- Span, R., Wagner, W.: A new equation of state for carbon dioxide covering the fluid region from the triple point temperature to 1100 K at pressures up to 800 MPa. *J. Phys. Chem. Ref. Data* **25**, 1509–1596 (1996)
- Span, R., Lemmon, E.W., Jacobsen, R.T., Wagner, W., Yokozeki, A.: A reference equation of state for the thermodynamic properties of nitrogen for temperatures from 63.151 to 1000 K and pressures to 2200 MPa. *J. Phys. Chem. Ref. Data* **29**, 1361–1433 (2000)
- Tegeler, C., Span, R., Wagner, W.: A new equation of state for argon covering the fluid region for temperatures from the melting line to 700 K at pressures up to 1000 MPa. *J. Phys. Chem. Ref. Data* **28**, 779–850 (1999)
- Touloukian, Y.S., Kirby, R.K., Taylor, R.E., Desai, P.D.: *Thermal expansion, metallic elements and alloys*. In: *Thermophysical Properties of Matter, the TPRC data series, vol. 12*. Plenum Press, New York (1975)
- Wagner, W., Kleinrahm, R.: Densimeters for very accurate density measurements of fluids over large ranges of temperature, pressure, and density. *Metrologia* **41**, S24–S39 (2004)
- Woltjer, H.R., Coppoolse, C.W., Wiersma, E.C.: On the magnetic susceptibility of oxygen as function of temperature and density. In: *Communication from the Physical Laboratory of the University of Leiden N° 201d*, pp. 1329–1333 (1929)
- Yang, X., Richter, M.: Experimental investigations of surface phenomena on porous and non-porous media near the dew points of pure fluids and fluid mixtures. *Langmuir* (2019)
- Yang, X., Richter, M., Wang, Z., Li, Z.: Density measurements on binary mixtures (nitrogen + carbon dioxide and argon + carbon dioxide) at temperatures from (298.15 to 423.15) K with pressures from (11 to 31) MPa using a single-sinker densimeter. *J. Chem. Thermodyn.* **91**, 17–29 (2015)
- Yang, X., Kleinrahm, R., McLinden, M., Richter, M.: Analysis of a commercial gravimetric sorption analyzer with simultaneous density measurement based on a magnetic-suspension balance: Uncertainties in sorption measurements. *Adsorption* (2019)

Publisher's Note Springer Nature remains neutral with regard to jurisdictional claims in published maps and institutional affiliations.